Published for SISSA by Springer

Received: July 27, 2015
Revised: October 12, 2015
Accepted: October 30, 2015
Published: November 30, 2015

Composite scalars at the LHC: the Higgs, the Sextet and the Octet

Giacomo Cacciapaglia,[a,e] **Haiying Cai,**[a,e] **Aldo Deandrea,**[a,b,e] **Thomas Flacke,**[c] **Seung J. Lee**[c,d] **and Alberto Parolini**[d]

[a] *Université de Lyon, France; Université Lyon 1, Villeurbanne, France*
[b] *Institut Universitaire de France, 103 boulevard Saint-Michel, 75005 Paris, France*
[c] *Department of Physics, Korea University, Seoul 136-713, Korea*
[d] *School of Physics, Korea Institute for Advanced Study, Seoul 130-722, Korea*
[e] *Institut de Physique Nucléaire de Lyon, CNRS/IN2P3, UMR5822, F-69622 Villeurbanne Cedex, France*

E-mail: g.cacciapaglia@ipnl.in2p3.fr, hcai@ipnl.in2p3.fr, a.deandrea@ipnl.in2p3.fr, flacke@korea.ac.kr, sjjlee@korea.edu, parloini85@kias.re.kr

Abstract: We present a phenomenological theory of scalar particles that transform as a sextet and an octet of QCD interactions. These particles may arise as light bound states of a fundamental dynamics giving rise to a composite Higgs boson and partial compositeness for the top. As a concrete example, we discuss an explicit UV completion based on the SU(4)/Sp(4) coset, where QCD colour is carried by additional fundamental fermions charged under the confining gauge group. Top partners, as well as potentially even lighter coloured scalars, arise as bound states of the coloured fermions. We study production and detection at LHC Run I and II of the octet and sextet, setting lower limits on masses and couplings to Standard Model particles using existing 8 TeV analyses. We finally explore prospects for the ongoing 13 TeV Run II: we focus on final states with two same sign leptons, that have the potential to discriminate the sextet.

Keywords: Beyond Standard Model, Technicolor and Composite Models, Global Symmetries

ArXiv ePrint: 1507.02283

doi:10.1007/JHEP11(2015)201

JHEP11(2015)201

Contents

JHEP11(2015)201

1 Introduction

The Higgs boson of the Standard Model (SM) and the associated mechanism for the electroweak symmetry breaking is a striking and remarkably successful description of the observed electroweak physics, starting from low energy data up to the high energy colliders such as LEP and the LHC. However, the quest for a more fundamental description of the electroweak and strong interactions is still wide open as not only fundamental theoretical questions await an answer, but also unexplained phenomena such as the origin of Dark Matter and the baryon asymmetry in the Universe. The two main avenues for physics beyond the SM lead to consider the Higgs boson either as a truly fundamental scalar particle as part of a larger fundamental sector (as in many supersymmetric or non-supersymmetric extensions of the SM), or as a composite state of a more fundamental underlying dynamics. The latter possibility is very intriguing as spontaneous symmetry breaking via confinement is a phenomenon which is observed in nature in many systems, notably in Quantum Chromo-Dynamics (QCD) in a relativistic system setup, as well as in non-relativistic cases, for example in condensed matter systems. Moreover, from the theoretical side, asymptotically free and confining theories have a special status as these theories are potentially well

defined at all scales. This second option is therefore theoretically appealing and was investigated in the past both at the effective and at the fundamental level. The earliest attempts in these directions were technicolor theories [1–3], which provided a simple testing ground for these ideas based on a scaled-up version of the QCD dynamics. It was soon clear that these first ideas needed to be implemented in a different way in order to allow for a light scalar boson. One key idea was to extend the global flavour symmetries of the underlying fermionic sector to generate a Higgs-like state as one of the pseudo-Nambu Goldstone Bosons (pNGB) of the theory, in a way similar to pions in QCD. In this way a composite scalar can be naturally and parametrically lighter than other composite particles in the theory [4–9]. More recently, models based on a warped extra dimensional background have been proposed and studied [10–12], while being conjectured to be dual descriptions of four-dimensional conformal field theories (holographic Higgs) [13]. The experimental discovery of a light Higgs boson at the LHC has further motivated the detailed study of models of composite pNGB Higgs, based on the effective chiral Lagrangian approach [14–21], mainly based on the minimal case that only contains a Higgs-like scalar as a light state. Chiral Lagrangians depend on the choice of the spontaneous global symmetry breaking pattern and fermion representations, but even if there are many possible choices for phenomenologically viable effective Lagrangians [22–24], it is not guaranteed that a fundamental UV description associated to a particular choice is possible in terms of a fundamental fermionic realisation. Therefore the effective chiral Lagrangian description of models of composite pNGB Higgs (usually called "composite Higgs models") do not provide a detailed understanding of the underlying physics. This is not a problem when trying to parameterise the Higgs sector, but one has to keep in mind that assumptions of what is the light sector of the theory are implicit in such a description. In particular the standard assumption of these models is that apart from the Higgs boson the next light states are fermionic top partners [25, 26]. One helpful approach to resolve this impasse is to consider a UV completion based on fundamental interactions and fermions [27], so as to complement and support the effective theory with a Fundamental Composite Dynamics (FCD) description. An alternative approach would be to rely on the existence of a conformal field theory in the UV, as described in the holographic approach. A number of recent papers have been dedicated to the FCD approach, providing a detailed description ranging from model building [27–33], lattice calculations [34], up to an overview of the phenomenology of the scalar and vector sectors [35]. More in general ref.s [36, 37] offer extensive and up to date reviews on model building efforts in the context of a composite Higgs.

In this paper we focus on a set of possibly light states that are usually not included in the chiral Lagrangian for composite models with top partners: scalar mesons that carry colour. Such states should actually be expected, as the FCD description necessarily couples to QCD colour if coloured fermionic resonances are expected to appear in the low energy regime: an effective theory of scalar leptoquarks in composite Higgs models with partial compositeness is presented in [38]. We will focus on a specific model proposed in [30], which relies on the coset SU(4)/Sp(4) to realize the pNGB Higgs. The SU(4)/Sp(4) coset is usually considered as the next to minimal "composite Higgs model" in the effective Lagrangian approach [23]. However this is a minimal choice when considering a description

JHEP11(2015)201

in terms of bound states of fermions [27, 29]. In this model the breaking is generated by an antisymmetric 6-dimensional representation (with respect to the global flavour symmetry) and the coset contains 5 Goldstone bosons. In terms of the custodial SO(4) subgroup of the residual symmetry group, the Goldstone bosons decompose into a $(\mathbf{2},\mathbf{2})+(\mathbf{1},\mathbf{1})$, which allows to obtain a pNGB Higgs. This case is also a simple example, which illustrates most of the important features of UV descriptions for FCD in the electroweak sector. In ref. [30], top partners, i.e. coloured fermionic bound states, are obtained by adding 6 additional Weyl fermions and thus enlarging the global symmetry of the model with an extra SU(6) which embeds the $SU(3)_c$ of QCD. At this point we notice that the FCD provides a genuine UV completion for the electroweak sector but it does not encompass a dynamical explanation for the couplings of the top partners to the top: while values for these mixings reproducing the correct top mass are certainly allowed we do not investigate under which conditions they are obtained. The only pragmatic assumption we make is that the scale at which the four fermion interactions responsible for the mixing are generated is at least larger than the natural cut-off of the effective field theory, $4\pi f$ where f is the scale of the condensate. For this case to happen, the operator mixing to the top needs to have large anomalous dimensions: having a detailed model for the underlying theory, in principle, allows to compute such anomalous dimensions (on the Lattice) and investigate the UV origin of the four fermion interactions. In this paper, however, we limit ourselves to an effective theory, where we take fully into account the symmetries of the underlying theory. We will focus, in particular, on the presence of coloured scalar resonances in the low energy theory. The breaking of the global SU(6) by an explicit mass term and the strong dynamics then implies the presence of 20 pNGBs in the spectrum, which decompose to a real colour octet and a complex charged sextet. After briefly discussing the connection between the masses of the coloured pNGBs and the masses of the top partners (which are needed to be light for naturalness arguments, and to generate the correct top mass), we consider the phenomenology of such states at the LHC. We consider in particular the case where they are the lightest composite coloured states in the spectrum, and then study the bounds from the LHC Run I data and the prospects to distinguish the presence of a sextet versus the octet at the LHC Run II. The analysis is done by using an effective description of their interactions, thus providing a model independent determination of their phenomenology.

The paper is organised as follows: in section 2 we discuss the structure of the model and its bound states. Section 3 is dedicated to constructing the effective description stemming from the fundamental model of a peculiar exotic scalar sextet which has potentially interesting collider signatures. Section 4 explores the signatures which are expected at the LHC for the exotic scalar sextets and octets present in the model and how to distinguish them in the LHC set-up. We discuss the conclusions which can be drawn on this class of models and the preliminary exploration of their phenomenology at the LHC in section 5.

2 The model: SU(4)/Sp(4) coset based on $G_{\mathbf{FCD}} = \mathbf{Sp}(2N_c)$

In order to explore the composite Higgs idea from the fundamental perspective of underlying constituent fermionic states, we consider a minimal model which was already outlined in

	$\mathrm{Sp}(2N_c)$	$\mathrm{SU}(3)_c$	$\mathrm{SU}(2)_L$	$\mathrm{U}(1)_Y$	SU(4)	SU(6)	U(1)
Q_1 Q_2	$\square$	**1**	**2**	0	**4**	**1**	$-3(N_c-1)q_\chi$
Q_3	$\square$	**1**	**1**	1/2			
Q_4	$\square$	**1**	**1**	$-1/2$			
χ_1 χ_2 χ_3	$\begin{smallmatrix}\square\\\square\end{smallmatrix}$	**3**	**1**	x	**1**	**6**	q_χ
χ_4 χ_5 χ_6	$\begin{smallmatrix}\square\\\square\end{smallmatrix}$	$\bar{\mathbf{3}}$	**1**	$-x$			

Table 1. Field content of the microscopic fundamental theory and property transformation under the gauged symmetry group $\mathrm{Sp}(2N_c)\times\mathrm{SU}(3)_c\times\ \mathrm{SU}(2)_L\times\ \mathrm{U}(1)_Y$, and under the global symmetries $\mathrm{SU}(4)\times\mathrm{SU}(6)\times\mathrm{U}(1)$.

the literature and partially explored in some of its phenomenological aspects. The model contains four Weyl techni-fermions Q_i in the spinorial representation of $\mathrm{Sp}(2N_c)$: the minimal choice is SU(2) with fermions in the fundamental [28, 29]. It has been shown on the lattice [34, 39, 40] that the global symmetry SU(4), acting on the Q's, is then dynamically broken to Sp(4), leading to five Goldstone bosons: three remain exact Goldstones and are eaten by the W and Z, one plays the role of the Higgs, and the fifth is a gauge singlet. Additional six techni-fermions χ_j in the 2-index anti-symmetric representation are needed to generate coloured fermionic bound states [30, 31], i.e. the top partners necessary to realize partial compositeness. This requirement imposes that the minimal FCD group is Sp(4), while larger FCD groups seem to be disfavoured: it has been shown that this model can satisfy electroweak precision tests [35] when the top partner sector is not included, and that it may be close to the conformal window once the χ's are added [41]. Larger N_c will lead to larger electroweak corrections, and to models that are deeper in the conformal window. Also vector and fermion resonances induce non negligible effects on precision parameters: in general they are model dependent and they can be large, potentially dangerous. Studies on models based on the minimal coset SO(5)/SO(4) show that there still exist available regions of parameter space, and therefore we expect the same to hold in the present case. The techni-fermions are charged under the FCD and SM gauge symmetries $\mathrm{Sp}(2N_c)\times\mathrm{SU}(3)_c\times$ $\mathrm{SU}(2)_L\times\ \mathrm{U}(1)_Y$ as reported in table 1.

With respect to the FCD, namely neglecting the SM gauging, the techni-fermions transform under a global symmetry $\mathrm{SU}(4)\times\mathrm{SU}(6)\times\mathrm{U}(1)$, with $\mathrm{SU}(2)_L\subset\mathrm{SU}(4)$, $\mathrm{SU}(3)_c\subset$ SU(6) and $\mathrm{U}(1)_Y\subset\mathrm{SU}(4)\times\mathrm{SU}(6)$. The SM hypercharge is obtained gauging a combination of a $\mathrm{U}(1)_x\subset\mathrm{SU}(6)$, and a U(1) included in the custodial $\mathrm{SO}(4)\subset\mathrm{SU}(4)$. The hypercharge x can be determined by the choice of which top partners couple with the top quarks. The global U(1) is the linear combination of Q and χ number which is not anomalous and whose charges are defined by $-3(N_c-1)q_\chi$.

JHEP11(2015)201

Here we will not study the details of the dynamics leading to the breaking of the global symmetries, as a discussion in terms of a Nambu-Jona-Lasinio model can be found in [30]: we will simply assume that both QQ and $\chi\chi$ form a condensate. Note that the value of the fermion bilinear operator on the vacuum will depend both on the spontaneous breaking induced by the strong dynamics and on explicit breaking terms, like the masses of the fundamental fermions. Once the gauge $\mathrm{Sp}(2N_c)$ interactions condense, two scalar bound states can form:

1. $\langle QQ\rangle$, transforming as $(\mathbf{6},\mathbf{1},2q_Q)$ under the flavour SU(4)×SU(6)×U(1) global symmetries. This object is the one responsible for the breaking of the SU(4) symmetry, and therefore the EW symmetry. The breaking pattern is SU(4)→ Sp(4). Note that this condensate will also break the global U(1).

2. $\langle\chi\chi\rangle$, transforming as $(\mathbf{1},\mathbf{21},2q_\chi)$ under the flavour symmetry. A non-zero value for its condensate corresponds to the mass term added in [30], i.e. a VEV for $\langle\chi\chi\rangle$. Thus, the mass term for the χ's explicitly breaks SU(6)→SO(6)∼SU(4). Note that SO(6) contains a subgroup $\mathrm{SU}(3)_c\times\mathrm{U}(1)_X$. This condensate also breaks the global U(1).[1]

2.1 Bound states

We can now classify all the bound states in terms of their transformation property under the global flavour symmetry SU(4)×SU(6), and their unbroken subgroups Sp(4)×SO(6) as shown in table 2. The SU(4) flavour symmetry is broken by the QQ condensate, which transforms as a 2-index anti-symmetric in flavour, i.e. as a **6** of SU(4). The breaking pattern is:

$$\mathrm{SU}(4)\to\mathrm{Sp}(4)\,,\quad \text{with}\ \ 15-10=5\ \ \text{pseudo-Goldstone bosons}\ (\pi). \tag{2.1}$$

For the SU(6) flavour symmetry, the condensate $\chi\chi$, transforming as a 2-index symmetric of SU(6), i.e. **21**, breaks

$$\mathrm{SU}(6)\to\mathrm{SO}(6)\,,\quad \text{with}\ \ 35-15=20\ \ \text{pseudo-Goldstone bosons}\ (\pi_c). \tag{2.2}$$

Note that the number of pseudo-Goldstones matches the dimensions of the π and π_c scalars. The 20 degrees of freedom in π_c correspond to the mesons R, P and $\tilde{P}$ in [30], while the singlet S is the analog of σ_c. Note also that the breaking of the global U(1) leads to an additional light singlet, which is a combination of σ and σ_c, while the orthogonal combination, being associated to the anomalous U(1), will develop a large mass (similarly to the η' in QCD).

The detailed spectrum of the low energy theory can only be studied numerically on the lattice. Naive expectation may lead us to guess that the pseudo-Goldstones π and π_c are parametrically lighter that the other states, while the scalar singlet, the spin-1/2 states and the vectors pick up a mass at the order of the condensation scales. As the

[1] Note that all χ's belong to the same representation of G_{FCD}, thus there is a global SU(6) symmetry rather than SU(3)×SU(3) [30]. The mass term can be expressed as a gauge-invariant combination of the χ's, which is invariant under a global SO(6).

JHEP11(2015)201

	spin	SU(4)×SU(6)	Sp(4)×SO(6)	names
QQ	0	$(\mathbf{6},\mathbf{1})$	$(\mathbf{1},\mathbf{1})$	σ
			$(\mathbf{5},\mathbf{1})$	π
$\chi\chi$	0	$(\mathbf{1},\mathbf{21})$	$(\mathbf{1},\mathbf{1})$	σ_c
			$(\mathbf{1},\mathbf{20})$	π_c
χQQ	1/2	$(\mathbf{6},\mathbf{6})$	$(\mathbf{1},\mathbf{6})$	ψ_1^1
			$(\mathbf{5},\mathbf{6})$	ψ_1^5
$\chi\bar{Q}\bar{Q}$	1/2	$(\mathbf{6},\mathbf{6})$	$(\mathbf{1},\mathbf{6})$	ψ_2^1
			$(\mathbf{5},\mathbf{6})$	ψ_2^5
$Q\bar{\chi}\bar{Q}$	1/2	$(\mathbf{1},\bar{\mathbf{6}})$	$(\mathbf{1},\mathbf{6})$	ψ_3
$Q\bar{\chi}\bar{Q}$	1/2	$(\mathbf{15},\bar{\mathbf{6}})$	$(\mathbf{5},\mathbf{6})$	ψ_4^5
			$(\mathbf{10},\mathbf{6})$	ψ_4^{10}
$\bar{Q}\sigma^\mu Q$	1	$(\mathbf{15},\mathbf{1})$	$(\mathbf{5},\mathbf{1})$	a
			$(\mathbf{10},\mathbf{1})$	ρ
$\bar{\chi}\sigma^\mu\chi$	1	$(\mathbf{1},\mathbf{35})$	$(\mathbf{1},\mathbf{20})$	a_c
			$(\mathbf{1},\mathbf{15})$	ρ_c

Table 2. Bound states of the model with spin and group properties with respect to the global flavour group and the unbroken subgroups.

SU(6) symmetry is broken explicitly by a mass term, the coloured pNGBs will be expected to have a mass of this order, however the χ mass will also contribute to a mass term for the spin-1/2 top partners. In fact, we can see from the table that it is not possible to write an SU(6)-invariant mass term for the composite fermions:[2] we can therefore guess that the mass of the fermions will receive contributions from the dynamical and explicit SU(6) breaking, while the pseudo-Goldstones π_c will only receive a contribution from the explicit breaking. On the other hand, the spin-1 states can have an SU(6) invariant mass. The expected hierarchy in the spectrum of coloured states is thus that the spin-1 are the heaviest states, while the π_c are the lightest.

This naive scenario can be altered when considering that the model is close to the conformal window, thus large anomalous dimensions may be generated for some of its composite operators. In particular, one may wish for a large anomalous dimension for the top partners, that brings down their mass close to 1 TeV in order to generate the correct top mass via partial compositeness. One qualitative argument is based on the observation that all top partners contain a QQ pair (in terms of the FCD, $\bar{Q}\bar{Q}$ is equivalent to QQ), which may be more tightly bound than the additional χ: in other words, we can assume for simplicity that the top partners are composed of a tightly bound QQ pair connected to a χ [30]. However, the QQ inside the top partners transforms as a 2-index antisymmetric of Sp($2N_c$), while the QQ pair that condenses is a singlet. We can then use the Maximally Attractive Channel (MAC) [42] reasoning: the force between two fermions

[2] We use Weyl fermion notation here, so a mass term will always be written as $\psi\psi'$, thus transforming as a $\mathbf{6}\otimes\mathbf{6}=\mathbf{21}\oplus\mathbf{15}$ of SU(6).

JHEP11(2015)201

in representations r_1 and r_2 of the strong dynamics which form a bound state in the r_{12} representation is proportional to

$$A = C_2(r_1) + C_2(r_2) - C_2(r_{12})\,, \tag{2.3}$$

thus the channel with larger A is more tightly bound. When combining QQ, the singlet channel (condensate) with $C_2(r_{12}) = 0$ is more attractive than the other one (QQ in the composite fermion) which has $C_2(r_{12}) > 0$. From this argument follows that the QQ pair inside the fermion is bound in a weaker way than the QQ pair in the condensate. One may therefore naively expect that the anomalous dimension of the QQ condensate is larger that the one of the top partners. Furthermore, all top partners in table 2 share the same structure in terms of the FCD as Q is in a pseudo-real and χ in a real representation, therefore the anomalous dimensions of the top partners should be very close to each other.

From the above arguments it follows that one may well expect that the dynamical mass of the top partners and of the scalars π_c are in the same ballpark. In the following, we will focus on this scenario, which contrasts with the choice made in [30] where the 6-plets $\psi_{1,2}$ made of χQQ bound states were chosen lighter than the other composite states, and the mesons π_c are considered much heavier. Note that the choice in [30] corresponds to the standard assumptions behind the model building of composite Higgs effective theories.

2.1.1 Mesons

The theory stemming from the structure we detailed above contains different bound state particles, which can be studied according to their statistics and their quantum numbers. A first class of particles are those analogous to the mesons which are found as bound states in strong interactions. In the limit where the condensates are aligned in a direction that does not break the SM gauge symmetries, we can use them to classify the various states. The mesons decompose as:

$$\begin{aligned}
\pi &= (\mathbf{1},\mathbf{2},\mathbf{2})_0 \oplus (\mathbf{1},\mathbf{1},\mathbf{1})_0\,,\\
\pi_c &= (\mathbf{8},\mathbf{1},\mathbf{1})_0 \oplus (\mathbf{6},\mathbf{1},\mathbf{1})_{2x} \oplus (\bar{\mathbf{6}},\mathbf{1},\mathbf{1})_{-2x}\,,\\
\sigma(\sigma_c) &= (\mathbf{1},\mathbf{1},\mathbf{1})_0\,;
\end{aligned}$$

where the representations under $\mathrm{SU}(3)_c\times\ \mathrm{SU}(2)_L\times\mathrm{SU}(2)_R$ are indicated by the numbers in parenthesis, and the subscript corresponds to the charge under $\mathrm{U}(1)_x$. We keep explicit track of the custodial symmetry embedded in the model, while the hypercharge $\mathrm{U}(1)_Y$ is the gauged subgroup of $\mathrm{SU}(2)_R\times\mathrm{U}(1)_x$.

The 5-plet π contains a bi-doublet that will play the role of the Brout-Englert-Higgs doublet, plus a singlet (η): once the condensate is misaligned in a direction that breaks the EW symmetry, the quantum numbers of the various states will not coincide any more with the quoted ones. Anyway, one can still think of the Higgs candidate as a leftover of the bi-doublet, while the singlet η will acquire some couplings to the SM gauge bosons. The phenomenology of the Higgs candidate and singlet states, in a model without top partners, has been studied in detail in [35]. The coloured scalars arise form the breaking of the SU(6) symmetry, necessary to give mass to the top partners without breaking any of the

JHEP11(2015)201

SM gauge symmetries: they will therefore play no role in the Higgs physics, however they will affect the phenomenology of the top partner sector, and they will be the focus of the present work. Other two scalars, σ and σ_c, are the pseudo Goldstone bosons of the $\mathrm{U}(1)_Q$ and $\mathrm{U}(1)_\chi$ associated to the Q and χ numbers, and they are SM singlets; a combination of the two gets mass via $\mathrm{Sp}(2N_c)$ instanton effects, corresponding to the anomalous global U(1). The orthogonal combination remains a pNGB, and receives a mass from the explicit breaking terms, like the masses of the fundamental fermions χ and Q.

Coloured pNGB masses. We now discuss more specifically the masses of the coloured pNGBs, which will be the object of the more detailed phenomenological analysis. The embedding of QCD $\mathrm{SU}(3)_c$ in the global SU(6) as in table 1 allows to write a mass term for χ as

$$\mathcal{L}_{\mathrm{FCD}} \supset m_\chi \, \chi^T \cdot \begin{pmatrix} 0 & 1_{3\times3} \\ 1_{3\times3} & 0 \end{pmatrix} \cdot \chi + h.c.\,. \tag{2.4}$$

The SU(3) preserving vacuum is therefore aligned with the mass matrix

$$\Sigma_{\chi\chi} = \begin{pmatrix} 0 & 1_{3\times3} \\ 1_{3\times3} & 0 \end{pmatrix}, \tag{2.5}$$

and it breaks $\mathrm{SU}(6) \to \mathrm{SO}(6)$, as expected. The unbroken gauged subgroup $\mathrm{SU}(3)_c \times \mathrm{U}(1)_x$ is thus

$$S^a = \frac{1}{\sqrt{2}} \begin{pmatrix} \lambda^a & 0 \\ 0 & -\lambda^{aT} \end{pmatrix}, \qquad X = x \begin{pmatrix} 1 & 0 \\ 0 & -1 \end{pmatrix}, \tag{2.6}$$

where λ^a are the Gell-Mann matrices (generators of $\mathrm{SU}(3)_c$). The coloured pions can be written as

$$U_6 = e^{i\Pi/f_6}\,, \qquad \Pi = \frac{1}{\sqrt{2}} \begin{pmatrix} \pi_8^a \lambda^a & \pi_6 \\ \pi_6^c & \pi_8^a \lambda^{aT} \end{pmatrix}, \tag{2.7}$$

where π_6 is a 3×3 symmetric matrix containing a complex colour sextet, and f_6 is the decay constant which is in general different with the decay constant f appearing in the QQ condensate. Note that the mass of the W and Z, and the scale of the electroweak symmetry breaking, are related to f.

Masses for the pions are generated by the explicit breaking terms of the global symmetry SU(6): the χ mass, gauge interactions and the couplings to the top. The contribution of the χ mass can be expressed as:

$$\mathcal{L}_{\mathrm{EFT}} \supset C_\chi m_\chi f_6^3 \,\mathrm{Tr}\left[\Sigma_{\chi\chi} \cdot U_6 \cdot \Sigma_{\chi\chi}\right] + h.c. \to M_\pi^2 \left(\frac{1}{2}\pi_8^2 + \pi_6^c \pi_6\right) + \dots \tag{2.8}$$

where $M_\pi^2 \sim C_\chi m_\chi f_6$, C_χ being a numerical factor. Gauge interactions contribute at one loop via the QCD

$$\mathcal{L}_{\mathrm{EFT}} \supset g_s^2 C_g f_6^4 \,\mathrm{Tr}\left[S^a \cdot U_6 \cdot \Sigma_{\chi\chi} \cdot (S^a \cdot U_6 \cdot \Sigma_{\chi\chi})^*\right] \sim C_g f_6^2 g_s^2 \left(\frac{3}{4}\frac{\pi_8^2}{2} + \frac{5}{6}\pi_6^c \pi_6\right) + \dots \tag{2.9}$$

JHEP11(2015)201

and $\mathrm{U}(1)_x$

$$\mathcal{L}_{\rm EFT} \supset g'^2 C_g f_6^4 \,\mathrm{Tr}\left[Y\cdot U_6\cdot \Sigma_{\chi\chi}\cdot (Y\cdot U_6\cdot\Sigma_{\chi\chi})^*\right] \sim C_g f_6^2 g'^2 2x^2\, \pi_6^c \pi_6 + \dots \tag{2.10}$$

contributions. The coefficients in front of the QCD loop can be easily understood in terms of the Casimir of the two representations: $C_2(\mathbf{8}) = 3$ and $C_2(\mathbf{6}) = 10/3$. Both contributions are expected to be positive, i.e. $C_\chi > 0$ and $C_g > 0$, else they would induce a VEV that breaks gauge interactions themselves. The contribution of top loops can be estimated by a spurionic analysis of the top couplings to the coloured pNGBs: all the composite baryons transform as the fundamental (or anti-fundamental) representation of SU(6), thus the elementary quark fields should be embedded in an anti-fundamental (or fundamental) in order for linear couplings to be written. We can thus associate the elementary fields to two spurions in, e.g., the $\bar{\mathbf{6}}$ of SU(6):

$$P_L^a = (0, \delta^{i,a})^T\,, \quad P_R^{\bar a} = (\delta^{j,\bar a}, 0)^T\,, \tag{2.11}$$

where a and $\bar a$ are indices of the QCD colour, and $i = 1,2,3$ and $j = 4,5,6$ run over the SU(6) indices. We can now build an operator, invariant under the stability group SO(6), as

$$\mathcal{O} = (U_6^\dagger \cdot P_X)^T \cdot \Sigma_{\chi\chi}\cdot U_8^\dagger \cdot P_Y\,, \quad X,Y = L,R\,. \tag{2.12}$$

The projectors P_X select a 3×3 sub-block of $\mathcal{O}$: the off-diagonal block, transforming as a $1\oplus 8$ of QCD colour, for L–R, the first diagonal block, transforming as a $\bar 6$, for R–R, and the second diagonal block, transforming as a 6, for L–L. The operator above can be used to construct effective couplings of the pNGBs to the tops, as follows:

$$\begin{aligned}
&c_{LR}\, v\, \left(1 - \tfrac{\sqrt{2}i}{f_6}\pi_8 - \tfrac{1}{f_6^2}\left(\pi_6\pi_6^c + \pi_8^2\right) + \dots\right) t_L t_R^c\,,\\
&c_{LL}\, \tfrac{v^2}{f}\left(-\tfrac{\sqrt{2}i}{f_6}\pi_6 - \tfrac{1}{f_6^2}\left(\pi_8\pi_6 + \pi_6\pi_8^T\right) + \dots\right) t_L^c t_L^c\,,\\
&c_{RR}\, f\left(-\tfrac{\sqrt{2}i}{f_6}\pi_6^c - \tfrac{1}{f_6^2}\left(\pi_8^T\pi_6^c + \pi_6^c\pi_8\right) + \dots\right) t_R t_R\,,
\end{aligned} \tag{2.13}$$

where the powers of v come from the SU(4)/Sp(4) structure and derive from the transformation properties of the top bilinear under $\mathrm{SU}(2)_L$ (we keep only the leading term in v/f), while the coefficients c_{XY} are quadratic in the pre-Yukawas and their form depends on the specific representation of Sp(4) the top partners belong to. The above formula is very general, and it only depends on the SU(6) representation of the top partners. The contribution to the pNGB masses can now be calculated by computing loops of the above operators: up to order $(v/f)^2$, we obtain

$$\delta m_{\pi_6}^2 = -\frac{\Lambda^2}{8\pi^2}\left(C_{RR}c_{RR}^2\frac{f^2}{f_6^2} - C_{LR}c_{LR}^2\frac{v^2}{f_6^2} + \mathcal{O}(v/f)^4\right)\,, \tag{2.14}$$

while no correction to the octet mass is generated. In the above formula, C_{RR} and C_{LR} are numerical $O(1)$ coefficients depending on the dynamics, and cut-off of the integral can be approximated by $\Lambda \sim 4\pi f$. This mass correction is expected to be negative.

All in all, the masses of the pions can be written as:

$$m_{\pi_8}^2 = M_\pi^2 + C_g f_6^2 \left(\frac{3}{4} g_s^2\right) , \tag{2.15}$$

$$m_{\pi_6}^2 = M_\pi^2 + C_g f_6^2 \left(\frac{5}{6} g_s^2 + 2x^2 g'^2\right) - C_{RR} f_6^2 c_{RR}^2 \frac{2f^4}{f_6^4} . \tag{2.16}$$

The mass hierarchy crucially depends on the size of the top loops:

$$m_{\pi_6}^2 - m_{\pi_8}^2 = -C_{RR} f_6^2 c_{RR}^2 \frac{2f^4}{f_6^4} + C_g f_6^2 \left(\frac{1}{12} g_s^2 + 2x^2 g'^2\right) . \tag{2.17}$$

If the top loop dominates, the sextet can be expected to be lighter than the octet Nevertheless this contribution can be made small in various ways: for instance, by reducing the coupling of the right-handed tops, or by generating a hierarchy $f < f_6$. The contribution of the gauge loops is more model independent, and it generates a numerically small mass splitting in favour of the octet.

2.1.2 Baryons (top partners)

A similar decomposition can be obtained for the fermionic bound states of the theory, among which one can identify the top partners involved in the generation of the top mass:

$$\begin{aligned}
\psi_{1,2}^{(1)} &= (\mathbf{3},\mathbf{1},\mathbf{1})_x \oplus (\bar{\mathbf{3}},\mathbf{1},\mathbf{1})_{-x} , \\
\psi_{1,2}^{(5)} &= (\mathbf{3},\mathbf{1},\mathbf{1})_x \oplus (\mathbf{3},\mathbf{2},\mathbf{2})_x \oplus (\bar{\mathbf{3}},\mathbf{1},\mathbf{1})_{-x} \oplus (\bar{\mathbf{3}},\mathbf{2},\mathbf{2})_{-x} , \\
\psi_3 &= (\mathbf{3},\mathbf{1},\mathbf{1})_x \oplus (\bar{\mathbf{3}},\mathbf{1},\mathbf{1})_{-x} , \\
\psi_4^{(5)} &= (\mathbf{3},\mathbf{1},\mathbf{1})_x \oplus (\mathbf{3},\mathbf{2},\mathbf{2})_x \oplus (\bar{\mathbf{3}},\mathbf{1},\mathbf{1})_{-x} \oplus (\bar{\mathbf{3}},\mathbf{2},\mathbf{2})_{-x} , \\
\psi_4^{(10)} &= (\mathbf{3},\mathbf{2},\mathbf{2})_x \oplus (\mathbf{3},\mathbf{3},\mathbf{1})_x \oplus (\mathbf{3},\mathbf{1},\mathbf{3})_x \oplus (\bar{\mathbf{3}},\mathbf{2},\mathbf{2})_{-x} \oplus (\bar{\mathbf{3}},\mathbf{3},\mathbf{1})_{-x} \oplus (\bar{\mathbf{3}},\mathbf{1},\mathbf{3})_{-x} .
\end{aligned}$$

Note that, if we choose $x = 2/3$, the fermion spectrum contains the following states:

- 4 t_L candidates contained in the bi-doublets $(\mathbf{3},\mathbf{2},\mathbf{2})_{2/3}$ which can mix with the elementary left-handed doublets: they are contained in $\psi_{1,2}^{(5)}$, $\psi_4^{(5)}$ and $\psi^{(10)}$;

- 7 t_R candidates: 6 in the form of $(\bar{\mathbf{3}},\mathbf{1},\mathbf{1})_{-2/3}$, present in $\psi_{1,2}^{(1)}$, $\psi_{1,2}^{(5)}$, ψ_3 and $\psi_4^{(5)}$, and one contained in the $\mathrm{SU}(2)_R$ triplet $(\bar{\mathbf{3}},\mathbf{1},\mathbf{3})_{-2/3}$ in $\psi_4^{(10)}$;

- 1 b_R candidate contained in the $\mathrm{SU}(2)_R$ triplet $(\bar{\mathbf{3}},\mathbf{1},\mathbf{3})_{-2/3}$ in $\psi_4^{(4)}$.

From this simple counting we can see that, while it would be possible in principle to give mass to all up-type quarks via partial compositeness, only one bottom state can receive its mass via this mechanism. In order to generate a sufficient number of partners for all SM quarks (and leptons), without changing the Higgs sector, the number of χ should be increased: besides the generation of many more fermionic and scalar states, the model would be more in danger of falling inside the conformal window. We will therefore consider here only the minimal case. A general study of the possible couplings in the fermionic sector

is beyond the scope of this work. A discussion of the possible role of various representations of the SU(4) flavour symmetry, for the purpose of giving mass to the top, can be found in [23]. We assume that some among these baryonic resonances couple linearly to left- and right-handed top, realizing the partial compositeness paradigm. These mixings are four fermion interactions in terms of the constituent fermions, generated at a certain scale. Notice that for this mechanism to work we need some physical process generating these interactions and proper values for couplings and anomalous dimensions so to reproduce the correct top mass: none of these is automatically in place in the present model. We put ourselves in the working assumption that suitable interactions are generated by a UV dynamics.

To counter the absence of partners for the light quarks and leptons, their masses can be generated assuming couplings of quark bi-linears with operators interpolating the Higgs field: in the UV they originate from four fermion interactions. If such terms are only needed to generate a mass as large as the charm in the up sector, and the strange in the down sector, while both top and bottom are partially composite, then it can be shown that no flavour symmetries are necessary to protect the model against flavour bounds [43]: this conclusion is general, and it does not depend on the representation of the multiplet the top (and bottom) partners belong to.

The model contains vector-like quark partners that arise as $\mathrm{SU}(2)_L$ and $\mathrm{SU}(2)_R$ singlets, doublets and triplets, with electromagnetic charges (when choosing $x = 2/3$) ranging from $-1/3$ to $5/3$. Vector-like quarks with such properties and coupling to third generation quarks have been extensively studied at the LHC, and after Run I their masses are constrained to be heavier than $\sim 700 - 900 \sim$ GeV (depending on the branching ratios into third generation quark and h, W, Z). In the same modes, a sensitivity up to ~ 1.4 TeV [44] (or even higher [45]) are to be expected for Run II. As in the model under consideration there are several top partners with the same electro magnetic charge, their signal cross sections for the respective final states add, such that bounds on the resonance mass can be expected to be larger.

2.1.3 Vectors (ρ and a)

Spin-1 bound states are a typical prediction of a large class of composite models and are also considered in effective chiral Lagrangian type models describing a composite or strongly interacting electroweak sector [46]. In the present model we have the following states:

$$\begin{aligned}
\rho &= (\mathbf{1},\mathbf{2},\mathbf{2})_0 \oplus (\mathbf{1},\mathbf{3},\mathbf{1})_0 \oplus (\mathbf{1},\mathbf{1},\mathbf{3})_0\,, \\
a &= (\mathbf{1},\mathbf{1},\mathbf{1})_0 \oplus (\mathbf{1},\mathbf{2},\mathbf{2})_0\,, \\
\rho_c &= (\mathbf{1},\mathbf{1},\mathbf{1})_0 \oplus (\mathbf{8},\mathbf{1},\mathbf{1})_0 \oplus (\bar{\mathbf{3}},\mathbf{1},\mathbf{1})_{2x} \oplus (\mathbf{3},\mathbf{1},\mathbf{1})_{-2x}\,, \\
a_c &= (\mathbf{8},\mathbf{1},\mathbf{1})_0 \oplus (\mathbf{6},\mathbf{1},\mathbf{1})_{2x} \oplus (\bar{\mathbf{6}},\mathbf{1},\mathbf{1})_{-2x}\,.
\end{aligned}$$

The ρ and ρ_c states correspond to "vector" resonances in QCD, transforming as the adjoint representation of the unbroken global symmetries, while the a and a_c correspond to the "axial" resonances, associated with the broken generators and thus transforming in the same representation as the pseudo-Goldstone mesons. Note that the ρ's contain a triplet

JHEP11(2015)201

of $\mathrm{SU}(2)_L$ and a triplet of $\mathrm{SU}(2)_R$, which can mix with the W and Z. These states can be constrained by perturbative unitarity and LHC direct search, like in minimal models [47–51]. The a's contain a 4-plet axial vector resonance. Its phenomenology related to Higgs decay is studied in a minimal SO(5)/SO(4) model [52]. ρ_c contains a "KK gluon", i.e. a colour octet cf. e.g. [53] for a recent study. This model also contains a colour sextet vector in the coset space, its collider simulation is explored in [54, 55]. The phenomenology of such states have been widely studied in the literature, and several searches from both ATLAS and CMS can be used to impose strict bounds on their masses, for example the recent experimental studies concerning same sign leptonic final states or multi-jet final states [56–63] which can be used to extract approximate bounds recasting these analyses. For the model presented here, these bounds apply only if the ρ_c states do not cascade decay through either top partners [64], or pseudo-goldstone bosons. Furthermore, the model under consideration contains additional states, like the "axial" colour sextet a_c, the colour triplet vectors, or the weak doublets, whose phenomenology deserves further studies.

Note, however, that spin-1 vectors are expected to be more massive than the meson bound states in the present class of models: this has been shown in the minimal model without top partners on the lattice [34, 40], where the spin-1 resonances appear at a scale above 3 TeV. In the present model, the near conformal dynamics may bring down the masses, however we would naively expect the hierarchy between masses, sketched above, to be preserved.

2.2 Couplings of the coloured pNGBs

The couplings of the coloured pions to fermions is relevant for the phenomenological study we perform in the following sections and can be obtained as follows. Consider generic composite top partner:

$$\Psi = \begin{pmatrix} \psi \\ \eta \end{pmatrix} \tag{2.18}$$

transforming as a $(\mathbf{R}, \mathbf{6})$ of the unbroken Sp(4)×SO(6) stability group. Here, ψ is a colour-triplet, while η is an anti-triplet, and both are left-handed Weyl spinors. This state can be embedded into an object transforming linearly under the full SU(4)×SU(6) group by inserting appropriate pion matrices:

$$\tilde{\Psi} = U_6 \cdot \begin{pmatrix} U_4^{(R)} \psi \\ U_4^{(R)} \eta \end{pmatrix} , \tag{2.19}$$

where $U_4^{(R)}$ is the pion matrix of SU(4)/Sp(4) in the representation $\mathbf{R}$ and U_6 is given in eq. (2.7). The linear mixing term of the left handed top with top partners can then be written as:

$$y_L f \, (0, \xi_L) \cdot \tilde{\Psi} = y_L f \left(1 - \frac{i}{\sqrt{2} f_6} \pi_8^a \lambda^{aT} \right) \xi_L U_4^{(R)} \eta - y_L f \, \frac{i}{\sqrt{2} f_6} \pi_6^c \xi_L U_4^{(R)} \psi + \dots \tag{2.20}$$

where ξ_L is the spurion containing the left-handed quarks in the representation $\bar{\mathbf{R}}$ of SU(4), and $(0, \xi_L)$ transforms as a $\bar{\mathbf{6}}$ of SU(6). Similarly, for right-handed quarks:

$$y_R f\,(\xi_R, 0)\cdot\tilde{\Psi} = y_R f\,\left(1 - \frac{i}{\sqrt{2}f_6}\pi_8^a\lambda^a\right)\xi_R U_4^{(R)}\psi - y_R f\,\frac{i}{\sqrt{2}f_6}\pi_6\xi_R U_4^{(R)}\eta + \dots \quad (2.21)$$

Note that the colour indices are omitted, and that the interactions with the un-coloured pions, the Higgs and the singlet η, arise form the expansion of the pion matrix $U_4^{(R)}$. This shows that the couplings of the octet and sextet are proportional to the pre-Yukawa couplings $y_{L/R}$ in the fermion sector.

As an explicit example, we will consider a set of composite fermions transforming as $\Psi = (\mathbf{6}, \mathbf{6})$ of SU(4)× SU(6), which decomposes as a $\mathbf{5}_{\mathrm{Sp}(4)}$ and a $\mathbf{1}_{\mathrm{Sp}(4)}$:

$$\Psi_5 = (\mathbf{5}, \mathbf{6})_{\mathrm{Sp}(4)\times\mathrm{SO}(6)}\,, \qquad \Psi_1 = (\mathbf{1}, \mathbf{6})_{\mathrm{Sp}(4)\times\mathrm{SO}(6)}\,. \quad (2.22)$$

This choice corresponds to mixing the tops with the composite baryon ψ_1, or ψ_2. In the vacuum where the EW symmetry is unbroken, the two composite fermions can be written in terms of an antisymmetric matrix in the Sp(4) space as follows:

$$\psi_5 = \begin{pmatrix} \frac{1}{2}\tilde{T}_5 i\sigma_2 & \frac{1}{\sqrt{2}}Q \\ -\frac{1}{\sqrt{2}}Q^T & \frac{1}{2}\tilde{T}_5 i\sigma_2 \end{pmatrix}, \quad Q = \begin{pmatrix} X_{5/3} & T \\ X_{2/3} & B \end{pmatrix}; \quad (2.23)$$

$$\eta_5 = \begin{pmatrix} \frac{1}{2}\tilde{T}_5^c i\sigma_2 & \frac{1}{\sqrt{2}}Q^c \\ -\frac{1}{\sqrt{2}}Q^{cT} & \frac{1}{2}\tilde{T}_5^c i\sigma_2 \end{pmatrix}, \quad Q^c = \begin{pmatrix} -X_{2/3}^c & B^c \\ X_{5/3}^c & -T^c \end{pmatrix}; \quad (2.24)$$

where the fields with a ^{c} are the change-conjugate of the right-handed chiralities. Note also that ψ_5 is a colour $\mathbf{3}$ with hypercharge 2/3, while η_5 is a colour $\bar{\mathbf{3}}$ with hypercharge −2/3. The singlet can be written as:

$$\psi_1 = \frac{1}{2}\tilde{T}_1\begin{pmatrix} i\sigma_2 & 0 \\ 0 & -i\sigma_2 \end{pmatrix}, \quad \eta_1 = \frac{1}{2}\tilde{T}_1^c\begin{pmatrix} i\sigma_2 & 0 \\ 0 & -i\sigma_2 \end{pmatrix}. \quad (2.25)$$

With this parametrisation, the masses of the two fermions can be written as

$$M_5\,\mathrm{Tr}[\eta_5\cdot\Sigma_B\cdot\psi_5\cdot\Sigma_B] + M_1\,\mathrm{Tr}[\eta_1\cdot\Sigma_B\cdot\psi_1\cdot\Sigma_B] + h.c. = \quad (2.26)$$

$$M_5(B^cB + T^cT + X_{2/3}^cX_{2/3} + X_{5/3}^cX_{5/3} + \tilde{T}_5^c\tilde{T}_5) + M_1\tilde{T}_1^c\tilde{T}_1 + h.c. \quad (2.27)$$

where

$$\Sigma_B = \begin{pmatrix} i\sigma_2 & 0 \\ 0 & -i\sigma_2 \end{pmatrix} \quad (2.28)$$

is introduced to properly contract the Sp(4) indices. The elementary SM fermions can be embedded in a spurion similar to ψ_5 for the left-handed doublets (t_L, b_L) and η_1 for the right-handed singlet t_R^c. We can now simply plug these matrices in the above formulas and

expand in the SU(4)/Sp(4) pseudo-Goldstone mesons (see appendix A for details). Putting the results together, in the basis $\{t, T, X_{2/3}, \tilde{T}_1, \tilde{T}_5\}$, the mass in the top sector is given by:

$$M_{\rm top} = \begin{pmatrix} 0 & y_{5L} f \cos^2\frac{\epsilon}{2} & -y_{5L} f \sin^2\frac{\epsilon}{2} & \frac{y_{1L} f}{\sqrt{2}}\sin\epsilon & 0 \\ \frac{y_{5R} f}{\sqrt{2}}\sin\epsilon & M_5 & 0 & 0 & 0 \\ \frac{y_{5R} f}{\sqrt{2}}\sin\epsilon & 0 & M_5 & 0 & 0 \\ y_{1R} f \cos\epsilon & 0 & 0 & M_1 & 0 \\ 0 & 0 & 0 & 0 & M_5 \end{pmatrix} . \tag{2.29}$$

One interesting feature is that the singlet $\tilde{T}_5$ does not mix with the other fields in the mass matrix. Additional couplings of the Higgs, in the form

$$i c_{L,R} \bar{\psi}_{5L,R} d_\mu \gamma^\mu \psi_{1L,R} = c_{L,R} \frac{\partial_\mu h}{2f} (\bar{T}_{L,R} + \bar{X}_{2/3L,R}) \gamma^\mu \tilde{T}_{1L,R} \,, \tag{2.30}$$

also do not explicitly involve $\tilde{T}_5$, thus we conclude that it does not mix with elementary fields at tree level even in the true mass basis. Therefore our set-up is similar to the minimal case SO(5)/SO(4) with $\mathbf{1} + \mathbf{4}$ top partners (known as MCHM5 [25, 65]). Once Yukawa couplings for the light quarks are turned on, the analysis carried on in [43] can be repeated here without major modifications: besides minor differences in the form of order one coefficients, as for instance the deviations of the couplings of the physical Higgs to fermions, the mass of the top can be obtained without violating flavour bounds.

Going in the mass eigenstate basis, at leading order in v/f, the couplings to top and bottom of the coloured mesons are:

$$i g_{\pi_8 t_L t_R^c} = \frac{m_{\rm top}}{f_6} \frac{2 + \cos(2\phi_L) + \cos(2\phi_R)}{2\sqrt{2}} + \dots \,, \tag{2.31}$$

$$i g_{\pi_6 t_R^c t_R^c} = \frac{M_1}{f_6} \frac{\sin^2\phi_R}{\sqrt{2}} + \dots \,, \tag{2.32}$$

$$i g_{\pi_6^c t_L t_L} = 0 + \dots \,, \tag{2.33}$$

$$i g_{\pi_8 b_L b_R^c} = 0 \,; \tag{2.34}$$

where

$$\tan\phi_L = \frac{y_{5L} f}{M_5} \,, \qquad \tan\phi_R = \frac{y_{1R} f}{M_1} \,. \tag{2.35}$$

The above coupling respect the form we anticipated in eq. (2.13).

As the pre-Yukawa couplings are required to be $\mathcal{O}(1)$ in order to obtain a large enough top mass, from the above results we can see that the sextet has $\mathcal{O}(1)$ couplings to the right-handed tops (mass eigenstates), while the couplings to the left-handed tops are suppressed by v^2/f^2. On the other hand, the couplings of the octet are suppressed by the top mass over the condensation scale. This result can be easily understood in terms of the EW quantum numbers of the states: the only gauge invariant combination of fermions that can form a sextet with charge 4/3 is a bilinear in the right handed tops, while all the other couplings need to be generated via the electroweak symmetry breaking source.

JHEP11(2015)201

2.3 Phenomenological considerations

As outlined earlier in this section, the model under consideration contains a large number of composite resonances: scalars, fermions and spin-1. Such states have been widely considered in phenomenological studies, however the interplay between them, in particular the scalar mesons and the fermionic baryons which are expected to be lighter, is still a fairly unexplored land.

The model we consider here, for instance, contains two un-coloured pNGBS: η and the singlet associated to the broken U(1) flavour symmetry. The phenomenology of the η has been discussed in ref. [35] in the absence of top partners. However, a natural expectation is that it is lighter than the top partners, thus they can decay into a SM quark plus η, providing final states not yet considered in experimental studies. A recent attempt to investigate the impact of η on the top partner searches has been presented in [66]. Similar impact may be expected from the singlet.

The coloured pNGBs are expected to have a similar mass as the top partners, thus their phenomenology crucially depends on the mass hierarchy. When they are lighter than the top partners, they may open a new decay mode for the top partners, thus affecting their phenomenology. For an inverted hierarchy, their decay into top partners become kinematically allowed, thus providing additional channels for single production of top partners. In the rest of this paper we will focus on the case where the mesons are lighter than the top partners, and we will only consider their direct production and decays into SM quarks. In section 3 we develop an effective field theory description which captures the main interactions of the sextet and octet states arising for example in the composite model discussed here. In section 4 we study the LHC phenomenology of the model. We then leave the investigation of their interplay with top partners to future work.

It should be noted that not all baryons need to couple to the SM quarks, so the possibility that some of them couple directly to a dark sector, not included in the model we present here, is viable. This case has been studied in general in [67].

3 Sextet effective theory

Studying the bound states of the FCD model with top partners in the previous section, we found that, apart from the baryonic top partners, other states with potentially interesting collider signatures can be present in the spectrum. Remarkably, one has scalar coloured mesons whose mass is expected at the same, if not lower, scale as the coloured baryons. In the specific model, the spectrum contains a complex colour sextet (with charge $Q = 4/3$) and a real colour octet. The presence of such states is rather generic, as any dynamics that generates coloured baryonic bound states is expected to contain also coloured mesons. In the rest of this paper, we will mainly focus on the possibility that such states are lighter than the fermionic states, thus they can only decay directly to a pair of SM particles.

In order to keep the discussion generic, we will study the constraints on a general Lagrangian. The couplings of the sextet and octet can be guessed by looking at the invariance under colour and charge: a sextet can only be obtained by combining two

JHEP11(2015)201

quarks, as for SU(3) representations $\mathbf{3}\otimes\mathbf{3}\supset\mathbf{6}$, or four anti-quarks $\bar{\mathbf{3}}\otimes\bar{\mathbf{3}}\otimes\bar{\mathbf{3}}\otimes\bar{\mathbf{3}}\supset\mathbf{6}$. Conversely, the octet can only couple to a quark-antiquark pair .

3.1 Baryon number conserving Lagrangian and couplings

An effective Lagrangian for the sextet and octet scalars can be easily build, by imposing invariance under colour and electric charge: we focus here on the case $x = 2/3$, for which the sextet has charge 4/3 and thus couples to a pair of up-type quarks. Below the EWSB scale, the effective Lagrangian reads

$$\begin{aligned}\mathcal{L} = &|D_\mu \pi_6|^2 - m_{\pi_6}^2 |\pi_6|^2 + \frac{1}{2}(D_\mu \pi_8)^2 - \frac{1}{2} m_{\pi_8}^2 (\pi_8)^2 - V_{\rm scalar}(\pi_6, \pi_8) \\ &+ a_R\ \pi_6 t_R^c t_R^c + a_L\ \pi_6^c t_L t_L + b\ \pi_8 t_R^c t_L + h.c. \end{aligned} \tag{3.1}$$

where $V_{\rm scalar}$ contains generic self-interactions between the scalars, and $t_{L/R}$ are chiral Weyl spinors (^{c} indicates the charge conjugation). Parity is in general not conserved in eq. (3.1), because only the coupling a_R corresponds to a gauge invariant operators, while the other couplings can only be generated via the EW symmetry breaking. In fact, one can expect

$$\frac{a_L}{a_R} \sim \mathcal{O}(v^2/\Lambda^2)\,, \quad \frac{b}{a_R} \sim \mathcal{O}(v/\Lambda)\,, \tag{3.2}$$

where Λ is the scale of new physics. This hierarchy of couplings is reflected in the explicit model discussed in the last section, where there $\Lambda = f$.

This Lagrangian is not the most general one because we couple the sextet only to the third generation quarks, while in principle we should take $a_{L,R}$ and b to be 3×3 matrices in family space: this choice can be motivated from a UV point of view, if top partners, and partial compositeness, is only invoked to give mass to top and bottom, while the light quarks, and leptons, receive their mass via bi-linear couplings. The robustness of this setup with respect to the experimental bounds on flavour observables has been studied in [43], where it was shown that this scenario passes all the bounds, without requiring special symmetries, independently on the coset and representations of the composite fermions: under the assumption of large enough anomalous dimensions of the bi-linear operators a high flavor scale is compatible with charm and bottom masses of the correct size, assuming also a near conformal behaviour between the two scales. The couplings to the coloured mesons are only generated for the top (and bottom) via the same mechanism giving them mass, while a coupling to the light quarks is induced once the quark fields are rotated in the true mass eigenbasis. However, a natural hierarchy between the contribution of the bi-linear couplings and the top mass ensues. The couplings in the mass basis, therefore, will be expressed in terms of mixing matrices of the form

$$a_L\, V_{uL}^{i3} V_{uL}^{j3}\,, \quad a_R\, V_{uR}^{*i3} V_{uR}^{*j3}\,, \quad b\, V_{uR}^{*i3} V_{uL}^{j3}\,, \quad \text{with} \quad i,j = 1,2,3\,. \tag{3.3}$$

The rotation matrices $V_{uL,R}$ are intrinsically hierarchical, due to the fact that the charm mass is generated by bi-linear interactions, while the top mass comes from partial compos-

iteness, thus we can estimate [43]

$$V_{uL,R} = \begin{pmatrix} O(1) & O(1) & O(\frac{m_c}{m_t}) \\ O(1) & O(1) & O(\frac{m_c}{m_t}) \\ O(\frac{m_c}{m_t}) & O(\frac{m_c}{m_t}) & O(1) \end{pmatrix} . \tag{3.4}$$

The couplings of the coloured mesons to light quarks are therefore strongly suppressed by powers of m_c/m_t, and are thus irrelevant for the phenomenology of these states at the LHC.

3.2 Flavour bounds

The exchange of coloured mesons can in principle generate large flavour changing neutral currents in the up-sector: the most dangerous one being the sextet which has couplings to the right-handed tops which is not suppressed by v/f. Flavour aspects in presence of scalar diquarks have been extensively investigated in [68]. The tree level exchange of π_6 scalars leads to four quark interactions. The induced operators has the form

$$\frac{|a_R|^2}{m_{\pi_6}^2}(t_R^c t_R^c)(t_R t_R) = \frac{|a_R|^2}{2m_{\pi_6}^2}(t_R^c \sigma^\mu t_R)(t_R^c \sigma_\mu t_R)\,, \tag{3.5}$$

where we used a Fierz-identity, and the colour indices are left understood. After rotating in the mass eigenstates, the operator $(c_R^c \sigma^\mu u_R)(c_R^c \sigma_\mu u_R)$, violating flavour number by two units, has a non zero coefficient given by

$$\frac{|a_R|^2}{m_{\pi_6}^2}\left(V_{uR}^{23\,*}\right)^2 V_{uR}^{13\,2} \sim \frac{10^{-9}}{(1\text{ TeV})^2}\left(\frac{|a_R|^2}{1}\right)\left(\frac{1\text{ TeV}}{m_{\pi_6}}\right)^2 . \tag{3.6}$$

The coefficient is experimentally bound to be less than 10^{-7} at the fixed reference scale of 1 TeV [69], thus giving a mild a_R-dependent bound on the mass of the sextet

$$m_{\pi_6} > 0.1\,|a_R|\,\text{TeV}\,. \tag{3.7}$$

An analogous operator is found with $R \to L$ and the experimental bound for it is of the same order [69, 70].

A further constraint on the flavour-conserving part of the operator can be obtained from the study of the angular distribution of dijet events at the LHC, which constrains the size of a generic four quark interaction. For operators

$$\frac{1}{M^2}(\bar{q}_X \gamma^\mu q_X)(\bar{q}_X \gamma_\mu q_X)\,, \quad q = u, d\,, \quad X = L, R\,, \tag{3.8}$$

$M > O(1)\,\text{TeV}$ is required [71, 72], where the precise value depends on the details of the operator. The operator generated in the model discussed in the last section is well below the bound thanks to the suppression from flavour mixing.

JHEP11(2015)201

3.3 Baryon number violation and neutron-antineutron oscillations

The model we introduced in section 2 is baryon number conserving: is suffices in fact to assign baryon number $3B = 1$ (-1) to the fundamental fermions χ transforming as a colour triplet (antitriplet), which translates in the sextet having baryon number $2/3$ and the octet carrying no baryon number. In general, however, one can write an additional operator coupling the sextet to down-type quarks:

$$\Delta\mathcal{L}_{\text{eff}} = c_R \; \pi_6 b_R b_R b_R b_R + h.c. \tag{3.9}$$

which is also unsuppressed by powers of v/Λ. The above operator has total baryon number 2 (note also that c_R has mass dimension -3). It cannot thus mediate the decay of the proton, however it will induce neutron-antineutron oscillations.

The current experimental limit, set by Super Kamiokande [73], on the period of neutron antineutron oscillations in empty space[3] is

$$\tau_{n-\bar{n}} \geq 2.44 \cdot 10^8 \; s \;\text{ at } 90\% \text{ C.L.} \tag{3.10}$$

This translates into a bound $\delta m \leq 10^{-33}\,\text{GeV}$ on the off-diagonal $n\bar{n}$ term in the effective 2×2 Hamiltonian for neutron oscillations [74]. In the SM Lagrangian the dimension nine operator

$$\frac{c_{\Delta B=2}}{M^5} uddudd \tag{3.11}$$

translates to

$$\delta m \sim c_{\Delta B=2}\Lambda_{QCD}\left(\frac{\Lambda_{QCD}}{M}\right)^5 = O(10^{-20}\text{ GeV})\left(\frac{c_{\Delta B=2}}{1}\right)\left(\frac{1\text{ TeV}}{M}\right)^5. \tag{3.12}$$

In the case under study, the coupling in eq. (3.9), together with the Lagrangian eq. (3.1), violates baryon number: integrating out at tree level the complex sextet π_6, and rotating in the mass eigenstate basis, we get, among others, the following dimension nine operator[4]

$$-\frac{a_R^* c_R^*}{m_{\pi_6}^2}(u_R)^p_{\dot{\zeta}}(d_R)^i_{\dot{\alpha}}(d_R)^k_{\dot{\gamma}}(u_R)^q_{\dot{\eta}}(d_R)^j_{\dot{\beta}}(d_R)^l_{\dot{\delta}}\epsilon^{\dot{\alpha}\dot{\beta}}\epsilon^{\dot{\gamma}\dot{\delta}}\epsilon^{\dot{\zeta}\dot{\eta}}\epsilon_{ikp}\epsilon_{jlq}(V_{uR}^{13})^2(V_{dR}^{13})^4\,, \tag{3.13}$$

which is of the form of eq. (3.11) with

$$\frac{c_{\Delta B=2}}{M^5} = -\frac{a_R^* c_R^*}{m_{\pi_6}^2}(V_{uR}^{13})^2(V_{dR}^{13})^4\,. \tag{3.14}$$

The hierarchic structure in the mixing matrices, eq. (3.4), implies then

$$\delta m = O(10^{-33}\text{ GeV})\left(\frac{a_R}{1}\right)\left(\frac{c_R}{(1\text{ TeV})^{-3}}\right)\left(\frac{1\text{ TeV}}{m_{\pi_6}}\right)^2, \tag{3.15}$$

compatible with the bound eq. (3.10) for $m_{\pi_6} \sim 1\,\text{TeV}$ and order one couplings.

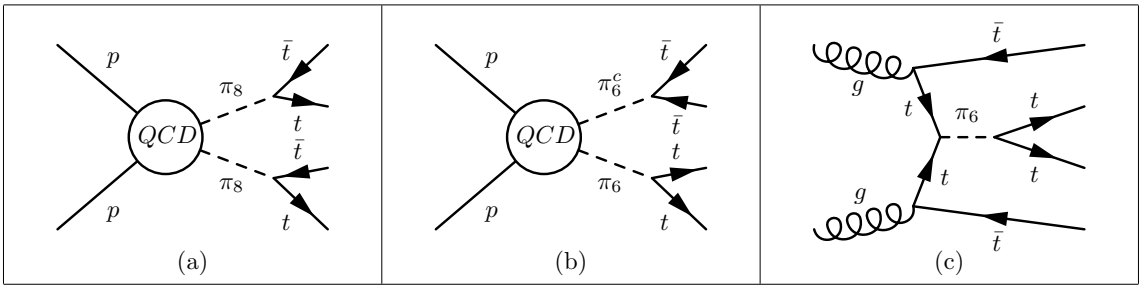

Figure 1. $tt\bar{t}\bar{t}$ production channels involving sextets and octets. The diagrams (a) and (b) show QCD pair production channels, where the QCD vertex includes the $gg\pi_{8,6}^c\pi_{8,6}$ interaction as well as an s-channel gluon (with gg or $q\bar{q}$ initial state) or a t-channel $\pi_{8/6}$ exchange with a gg initial state. Figure (c) shows the $tt\bar{t}\bar{t}$ contribution from π_6 single production. The single π_6^c production contribution is obtained analogously (with $t \leftrightarrow \bar{t}$ and $\pi_6 \to \pi_6^c$).

4 LHC phenomenology of the sextet and octet

The Run II at the LHC is an extremely important opportunity to test the presence of exotic particles predicted by the class of composite models we are considering, especially regarding coloured states. Early stage studies for pair and single production of the coloured scalars (triplet, sextet and octet) can be found in the literature [75–77]. Here we will focus on the case where the coloured states couple mainly to tops, which is relatively easy to probe at the LHC. Four top quark events are a particularly attractive channel, as the production rates in the SM are very small (of the order of 1 fb at $\sqrt{s} = 8$ TeV for the LHC), while they can be significantly enhanced in extensions of the SM, as studied for various particle physics scenarios [78–82] and searched for by ATLAS and CMS [83–88].

Existing bounds from LHC Run I. Given the specific couplings predicted in the composite model we consider, there are four main channels contributing to the $tt\bar{t}\bar{t}$ final state, which include the single and pair sextet production, i.e. $pp \to \bar{t}\bar{t}\pi_6$, $tt\pi_6^c$, $\pi_6\pi_6^c$, with $\pi_6 \to tt$, and also the pair octet production, i.e. $pp \to \pi_8\pi_8$, with $\pi_8 \to t\bar{t}$ (cf. figure 1).[5] We first use the analysis of same sign dilepton (2SSL) at 8 TeV to extract a bound on the mass of the coloured scalar resonances, assuming equal masses $m_{\pi_6} \approx m_{\pi_8} \approx M_\pi$. The cross section at the leading order for each channel at a 8 TeV LHC is shown in the left panel of figure 2, together with the experimental bound. Considering the contribution from all the important channels, a sextet and octet with masses smaller than ~ 800 GeV are disfavoured by the 2SSL analysis, done with the full Run I data of 20.3 fb^{-1}, by the ATLAS collaboration [87]. The recent ATLAS search [88] in the lepton-plus-jets final state, also on the full Run I data, yields a more stringent bound for the $4t$ cross section: comparing this bound with the model cross sections, as shown in the right panel of figure 2, implies

[3]This measure is extracted looking at oscillations in nuclei. The conversion to the free case is obtained estimating a nuclear suppression factor.

[4]Here, $\alpha, \beta = 1, 2$ are spinor indices and $i, j = 1, 2, 3$ $\mathrm{SU}(3)_c$ indices.

[5]We neglect here the single octet production $pp \to t\bar{t}\pi_8$, as this process is suppressed by a factor of $m_t^2/M_1^2 \sim \mathcal{O}(10^{-2})$ from the octet coupling, compared with the process with single sextet production.

JHEP11(2015)201

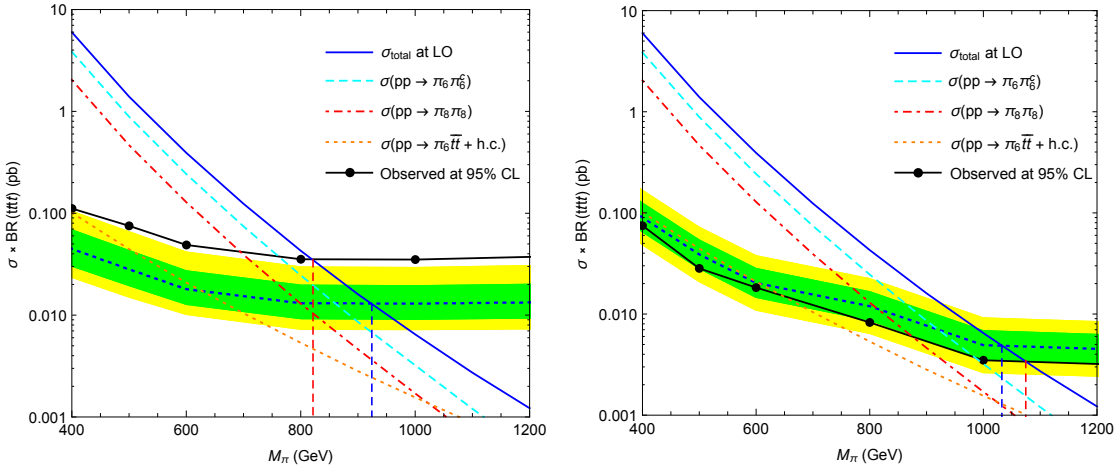

Figure 2. Cross sections for the sextet and octet scalars at the LHC at 8 TeV, with $a_R = 1$. Left panel: comparison with the ATLAS 2SSL search [87], where the green (yellow) band is for 1σ (2σ) expected limit and the solid black curve is the observed limit. Right panel: comparison with the ATLAS 1-lepton search observed limit [88].

a limit of $M_\pi \gtrsim 1.1$ TeV. The single-lepton analysis, however, relies on a shape fit on a kinematical distribution (H_T) in a region where very few events are present. We therefore decided to rely on the 2SSL analysis, which is a robust cut-and-count search, to set the lowest acceptable mass value for the coloured scalars.[6] In the comparisons of the cross section in figure 2 to the ATLAS studies, we are assuming that the efficiency of the signal selection is the same as the one obtained by ATLAS on the octet pair production signal: in the 2SSL analysis, one might expect some differences as the leptons arising from $\pi_6 \to tt$ decays have different kinematics. For the single lepton analysis the assumption of same efficiencies is fully justified as the search is blind to the charge of the t vs. $\bar{t}$ such that $\pi_8 \to t\bar{t}$ and $\pi_6 \to tt$ do not lead to distinguishable topologies for this search.

The leading order cross sections at the Run II LHC with $\sqrt{s} = 13$ TeV is shown in figure 3, with the π_6-t-t coupling set to one. As can be seen, for this coupling value the single π_6 production cross section becomes larger than the octet π_8 pair production cross section at $M_\pi > 1.2$ TeV. Note that in computing the cross sections of figure 2 and 3, and all the numerical results in this section, we are using results at leading order. Next-to-leading order corrections, expressed in terms of k-factors, for the octet pair production have been calculated in [91], and are found to be close to unity for M_π above a TeV. The k-factors for the sextet single and pair production are not available in the literature. For

[6] CMS performed a search for four tops in the lepton-plus-jets final state which yields an upper bound of 32 fb^{-1} at 95% c.l. on the four-top production cross section [86]. As this study focusses on SM-like four-top signatures, the bounds from it on colour sextets and octets are weaker than the one of the ATLAS study used here. CMS also performed a search in the 2SSL and b-jets channel [89] and the 2SSL and jets channel [90], which are tailored for supersymmetric model signatures and yield upper bound of 49 fb^{-1} at 95% c.l. on the four-top production cross section. This bound resembles the ATLAS search bound of [87], although the bounds cannot be compared directly as they have been determined based on different underlying model assumptions.

JHEP11(2015)201

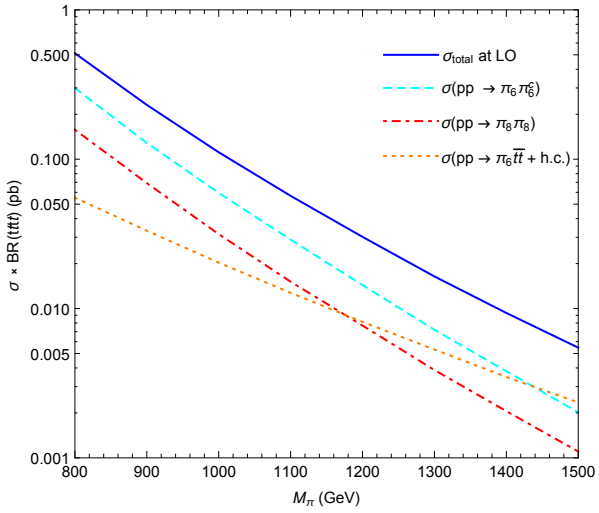

Figure 3. Cross sections for the sextet and octet scalar production at the LHC 13 TeV, with $a_R = 1$.

pair production of the sextet, the k-factors can be expected to be similar to the octet ones, i.e. close to unity, such that our pair production channels should be well approximated when treating them at leading order. For the π_6 single production, k-factors may be very different: however, this production channel depends on the free coupling π_6-t-t such that — at least for the overall cross section — a k-factor can be effectively absorbed into the definition of the coupling a_R appearing in the leading order calculation.

Simulation for LHC Run II. Both the single and pair production of π_6 and π_8 yield $tt\bar{t}\bar{t}$ final states for which — as it has been found at the LHC Run I — the 2SSL and the single lepton-plus-jets channels provide strong discovery potential. To distinguish sextet and octet signals, however, the 2SSL channel is more promising. The sextet decays to a same sign tt pair, while the octet decays to $t\bar{t}$. Thus, in a 2SSL search, the two same sign leptons arise either from the decay of the same particle (π_6 or π_6^c) or from two different particles (in the case of $\pi_8\pi_8 \to t\bar{t}t\bar{t}$), implying very different kinematical distributions for the 2SSL in the two cases. In the following we outline a cut-scheme to isolate sextet and octet searches from SM background and then explore how kinematic differences of sextet and octet signatures might be used in order to disentangle π_6 and π_8, in case an excess is observed at the Run II.

The 2SSL signature we base our study on arises from a final state with 4 $b + \ell^\pm\ell^\pm +$ 4 $jets + \not{E}_T$, where the two leptons come from the leptonic decays of two same sign tops, while the remaining two tops decay hadronically. For the object selection at 13 TeV, we adopt kinematic cuts similar to the ones described in the ATLAS search for 2SSL signature at 8 TeV [85], but for simplicity we impose identical pseudo-rapidity (η) cuts on electrons and muons, without excluding the "crack" region $1.37 < |\eta| < 1.52$ for electrons. This simplified treatment will lead to a discrepancy in the acceptance of up to 3%, which is negligible to other intrinsic uncertainties in our simulation. Moreover, we propose to

JHEP11(2015)201

include several additional critera, e.g. ordering the hard jets and requiring veto cuts for an additional lepton, in order to increase the yield of signal/ background and to optimise the possibility to search for sextet and octet scalars. The following event-selection criteria are imposed for leptons and jets in order to perform a detailed analysis of the LHC prospect for searching this specific signature:

1. We demand at least two b-tagged jets, where we assume $\simeq 70\%$ tag rate for a b-jet, $\simeq 8\%$ mistag rate for a c-jet, and a flat $\simeq 1\%$ mistag rate for a light quark or gluon without accounting for its p_T dependence. For the signals with four top quarks (and therefore four b-jets), the signal efficiency of this cut is high ($\sim 92\%$) while backgrounds with two top quarks are reduced by 50%.

2. We demand 2SSL with positive charge, l^+l^+, and transverse momentum $p_T^\ell > 24$ GeV, and pseudo-rapidity $|\eta_\ell| < 2.5$. We specify the 2SSL charge here because l^+l^+ can only arise from two tops (but not anti-tops) which can for example arise from the decay of a π_6 (but not a π_6^c). The following discussion can be repeated for the l^-l^- channel in complete analogy, when replacing tops with anti-tops, π_6 with π_6^c, W^+ with W^-, etc.

3. We require at least 4 additional jets with $p_T^j > 24$ GeV, and $|\eta_j| < 2.5$. With the jet number cut condition $N_j \geq 4$, we can safely ignore SM background from diboson processes, i.e. WZ, ZZ and W^+W^-+2 jets.

4. As separation criteria, we demand $\Delta R_{jj} > 0.4$, $\Delta R_{j\ell} > 0.4$, and $\Delta R_{\ell\ell} > 0.4$, with $\Delta R = \sqrt{(\Delta\eta)^2 + (\Delta\phi)^2}$ being the angular separation between two observable particles.

5. To account for the neutrinos, we impose a missing transverse energy cut: $\not{E}_T > 40\,\text{GeV}$.

6. We order the additional jets (except the two tagged bottom quarks) in p_T^j and require that the leading jet satisfies $\max(p_T^j) > 100\,\text{GeV}$, and the subleading jet satisfies $\max(p_T^j) > 50\,\text{GeV}$. In figure 4, we show that this cut has a minor effect on the signal while reducing the background by 50%.

7. Finally, we demand $H_T > 650\,\text{GeV}$, where $H_T = \Sigma p_T^\ell + \Sigma p_T^j$ is the scalar sum of all jet and lepton transverse momenta. The distribution of $\not{E}_T$ and H_T are shown in figure 5 which show that only H_T has a good discrimination power for signal events from the SM background.

The signal events for sextet and octet as well as the dominant SM backgrounds ($t\bar{t}W^\pm$+jets, $t\bar{t}Z$+jets, $t\bar{t}W^+W^-$, and $t\bar{t}t\bar{t}$) at 13 TeV are generated by MadGraph 5.2 [92] with the parton distribution function (PDF) MSTW2008NLO [93]. The renormalisation and factorisation scales are set to $\mu_F = \mu_R = 1/2 \sum_f m_f$, where we sum over the mass of the final state particles. Note that we do not consider backgrounds arising from "fake" leptons and charge mis-identification, as such background can only be reliably estimated

JHEP11(2015)201

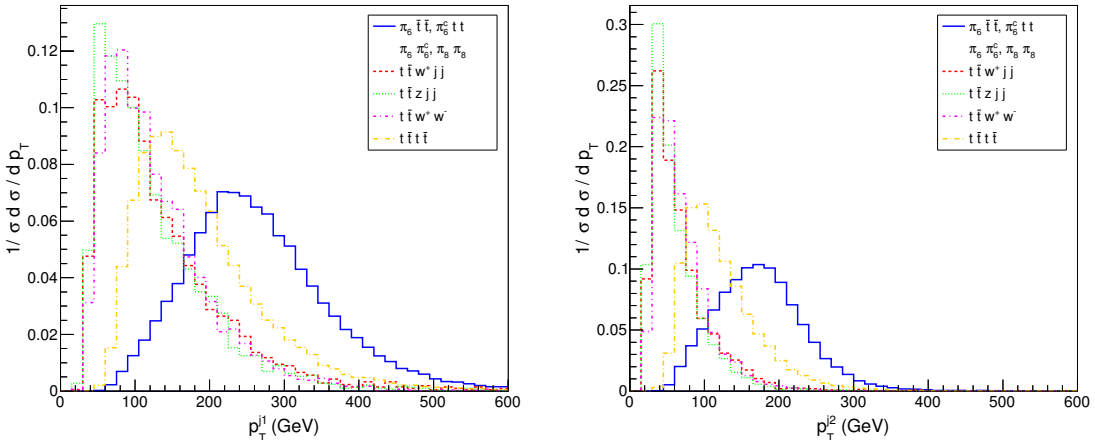

Figure 4. p_T distributions for the main backgrounds and for the signal (the sum of the $\pi_6\overline{tt}, \pi_6^c tt, \pi_6^c\pi_6$, and $\pi_8\pi_8$ channels). The left panel shows the leading jet and right panel shows the subleading jet p_T distribution after the basic cuts.

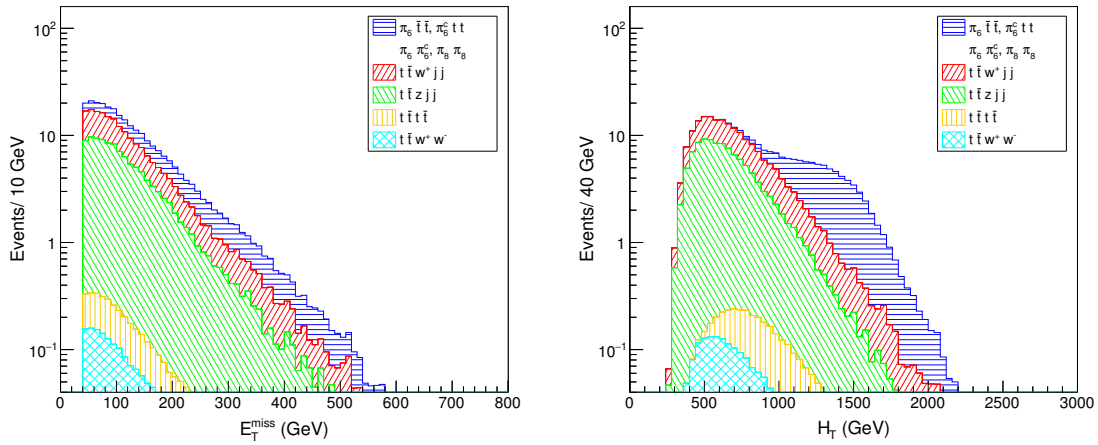

Figure 5. Left panel: staggered plot of the missing energy ($\not{E}_T$) distribution of the main backgrounds and the sum of the signal channels. Right panel: staggered plot of the H_T distribution of main backgrounds and the signal. The masses of sextet and octet are assumed to be equal $M_\pi = 900\,\text{GeV}$, and the coupling π-t-t is set to be $a_R = 1$. The events are selected after the basic cut, with the b-tag efficiency included.

from the data. We do not use our background simulation in order to estimate discovery or exclusion potentials, here, and provide the SM backgrounds only in order to motivate the cuts chosen and to determine realistic signal efficiencies.

The numbers of events after each cut are shown in table 3. The row "no cut" corresponds to a mild kinematic cut $p_T^j > 10\,\text{GeV}$ for the light jets, but zero p_T cuts for both the leptons and bottom quarks. The basic cuts in the second row include the event selection (1–5). The acceptances after passing all the selection criteria is reported in the bottom

JHEP11(2015)201

	$t\bar{t}W^+jj$	$t\bar{t}Zjj$	$t\bar{t}W^+W^-$	$t\bar{t}t\bar{t}$	M_π (TeV)		
					0.9	1.0	1.2
no cut	800	787	11.4	7.40	192	85.0	19.1
basic cuts (1–5)	85.1	107	1.60	2.05	64.5	26.7	5.16
$p_T^{j1} > 100$ GeV, $p_T^{j2} > 50$ GeV ($p_T^{\ell^-} < 10$ GeV, or $\lvert\eta_{\ell^-}\rvert > 2.5$)	36.4	2.03	0.72	1.83	63.4	26.1	5.0
$H_T > 650$ GeV	28.1	1.36	0.51	1.68	63.2	26.0	4.99
Acceptance	3.5%	0.17%	4.5%	23%	33%	31%	26%

Table 3. Number of events and final acceptance for the main SM backgrounds (not including fakes and charge mis-id) and for the signal from single and pair productions of $p\,p \to \bar{t}\bar{t}\pi_6$, $tt\pi_6^c$, $\pi_6\pi_6^c$, $\pi_8\pi_8$ in an effective model with $a_R = 1$. Numbers are given for an integrated luminosity of $\int Ldt = 100$ fb^{-1} at a $\sqrt{s} = 13$ TeV LHC.

	M_π	0.9 TeV	1.0 TeV	1.1 TeV	1.2 TeV	1.3 TeV	1.4 TeV	1.5 TeV
	$\pi_8\pi_8$	18.6	7.60	3.06	1.25	0.55	0.23	0.10
$a_R = 1$	$\pi_6\pi_6^c$	35.3	13.1	4.99	1.99	0.81	0.32	0.14
	$\pi_6\bar{t}\bar{t}$	4.89	2.93	1.75	1.01	0.60	0.36	0.22
	$\pi_6^c tt$	4.38	2.40	1.35	0.74	0.42	0.25	0.15
$a_R = 2$	$\pi_6\pi_6^c$	24.2	9.67	4.02	1.76	0.80	0.36	0.18
	$\pi_6\bar{t}\bar{t}$	16.8	10.5	6.47	4.02	2.62	1.72	1.14
	$\pi_6^c tt$	15.1	8.76	5.30	3.38	2.08	1.35	0.94

Table 4. Number of events for each channel with an integrated luminosity $\int Ldt = 100$ fb^{-1} at Run II after cuts. For the sextet, we used $a_R = 1$ (upper block) and $a_R = 2$ (lower block).

row of the table. As can be seen, the signal acceptance decreases with increasing sextet and octet mass. In table 4 we provide a more detailed overview of the expected number of events from different signal channels for various masses and two values of the coupling a_R. We checked that for $a_R \leq 1$, the narrow width approximation holds, so that smaller values of a_R can be easily obtained by rescaling the yield in single production by a factor a_R^2. For larger values of a_R, the narrow width approximation starts breaking down, and one can see effects in the efficiency due to the different kinematics of the decay products. This is illustrated at the point $a_R = 2$: the large width affects the kinematic distributions so that the signal yield in the pair production is reduced, while for the single production we see that the yield is larger than the naive factor of 4 for light masses ($M_\pi \leq 1.2$ TeV), while it is reduced at large masses.

In the simulation we only included true SM backgrounds for the 2 b + 2 SSL + multi-jets signature, as fakes and charge misidentification can only reliably estimated with data based techniques. The list of the considered backgrounds, and their treatment, follows:

- $t\bar{t}W^\pm$ + jets: as we choose two positive leptons as the signature, we are interested in the final states with $t \to b\ell^+\nu_\ell$, $\bar{t} \to \bar{b}jj$ and $W^+ \to \ell^+\nu_\ell$. This process represents the most sizable background for our signature.

- $t\bar{t}Z$ + jets: this process yields a background for our signal if $t \to b\ell^+ v_\ell$, $\bar{t} \to \bar{b}jj$ and $Z^+ \to \ell^+\ell^-$. In addition to the basic cut, we veto negatively charged electrons which have either $p_T > 10$ GeV or $\eta_\ell < 2.5$. This veto cut is crucial in our search strategy as it efficiently suppresses the $t\bar{t}Z$ background. While without this cut, the $t\bar{t}Z$ background efficiency is similar to the $t\bar{t}W$ one (which is around 3.5%), the veto reduces the $t\bar{t}Z$ acceptance to negligible 0.17%.

- $t\bar{t}W^+W^-$: this process yields a background if top and W^+ decay leptonically such that they generate the 2SSL. The anti-top and W^- need to decay hadronically to produce additional jets to pass the event selection. The SM cross section for this process is small due to one additional massive gauge bosons present in the final state.

- four top production $t\bar{t}t\bar{t}$: this process corresponds to our signal final state, thus it is irreducible and has high efficiency. However, the SM cross section of the process is small ($\sim$ two orders of magnitude lower than the cross section before cuts of the dominant background $t\bar{t}W^\pm$+jets), such that its final contribution to the background is subdominant.

Distinguishing sextets from octets. Assuming that the LHC will collect enough statistics at Run II to see an excess in the 2SSL channel, one may ask the question if the signal is due to an octet or a sextet. The crucial difference between sextets and octets in the 2SSL search is that for sextets the SSLs originate from $\pi_6 \to tt \to (l+\bar{\nu}b)(l+\bar{\nu}b)$, i.e. from the same resonance while for octets, each lepton originates from a top which result from the decay of two $different$ π_8 resonances. This difference manifests itself very clearly in the angular distributions of the leptons and in the resonances' mass reconstruction, as we shown the following.

Starting with the mass reconstruction, let us first consider an l^+l^+ signal arising from octet pair production. Reconstructing the π_8 mass requires to identify the correct combinations of $t_1\bar{t}_1 \to (l^+\bar{\nu}b)_1(\bar{b}jj)_1$ and $t_2\bar{t}_2 \to (l^+\bar{\nu}b)_2(\bar{b}jj)_2$. The reconstruction of semi-leptonic $t\bar{t}$ resonances is commonly applied, for example in Z' or KK-gluon searches (although these searches only reconstruct one $t\bar{t}$ pair and not two as present in our case). For recently applied search strategies at ALTAS and CMS cf. e.g. [94, 95].

For the mass reconstruction of the sextet from the 2SSL channel with l^+l^+, one can hope to reconstruct both the invariant mass of the leptonically decaying pair of tops (originating from $\pi_6 \to tt$ in our sample with l^+l^+ pairs), and of the hadronically decaying ones (arising from $\pi_6^c \to \overline{tt}$ in our sample).

The hadronically decaying resonance in l^+l^+ searches appears in the production channels of $pp > \pi_6\pi_6^c$, $tt\pi_6^c$ from decays of the resonance π_6^c, while the other channels act as backgrounds. To reconstruct the 6-jet resonance we first pick two jets whose combined invariant mass lies in the window of $|m_{j_1j_2} - m_W| < 10$ GeV and identify them as a hadronic W. Next, we use another mass window criterion $|m_{j_3W} - m_t| < 10$ GeV to select a third jet or b-jet, which we pair with the reconstructed W bosons to an anti-top quark candi-

date.[7] Applying the same procedure to the remaining jets and b-jets gives rise to another W^- and anti-top reconstruction. Thus the four momentum of the π_6^c particle can be fully reconstructed from the hadronically decaying anti-tops as $p^\mu_{\pi_6^c} = p^\mu_{\bar{t}} + p^\mu_{\bar{t}}$.

The positively charged di-leptons arise from the processes $pp > \pi_6\pi_6^c$ and $\bar{t}t\pi_6$, where π_6 decays to 2 b, 2 SSL plus $\not{E}_T$.[8] The reconstruction procedure for the leptonically decaying top pair is much more complicated due to the missing energy from the two neutrinos. In the event selection, we demand 6 jets, two b-tagged jets, and 2 positive leptons. With the reconstruction of the two hadronic anti-tops, only two (possibly b-tagged) jets and the leptons remain which are the b's and leptons from the two top decays in the underlying event. We face the problem to correctly combine the b's with the leptons to a (b_1, ℓ_1) pair from one decay chain and the (b_2, ℓ_2) from the other one. We will demonstrate that the m_{T2} variable can be used to identify the correct combination in an very efficient way compared with other possible variables, e.g. the invariant mass of the (b_1, ℓ_1) cluster. The kinematic variable m_{T2} is defined in analogy to the transverse mass, but extended to the case with two missing particles [96, 97]. For events with two missing particles with mass μ_N in two identical decay chains, the quantity m_{T2}^2 is evaluated as the minimum of transverse mass square over all partitions of the measured $\not{p}_T$, i.e.

$$\min_{\not{p}_T^1 + \not{p}_T^2 = \not{p}_T} \left[\max\{ m_T^2(p_T^a,\ \not{p}_T^1;\ \mu_N),\ m_T^2(p_T^b,\ \not{p}_T^2;\ \mu_N) \} \right], \tag{4.1}$$

where the transverse mass square m_T^2 is defined as:

$$m_T^2(p_T^a,\ \not{p}_T^1;\ \mu_N) = m_a^2 + \mu_N^2 + 2(E_T^a\ \not{E}_T^1 - p_T^a \cdot\ \not{p}_T^1) \tag{4.2}$$

with p_T^a being the transverse momenta of a visible cluster in one decay chain. In our case, we set $p_T^a = (p_{b_1}^x + p_{\ell_1}^x, p_{b_1}^y + p_{\ell_1}^y)$ and $\mu_N = 0$ since the neutrino mass is zero. As shown in the left panel of figure 6, for the correct assignment of the $(b\text{-}\ell^+)$ cluster, m_{T2} peaks around the top quark mass, while for the "wrong" combination its value is generally larger than the top quark mass and peaks at a much higher energy scale. Thus in the simulation, we identify the combination (b_1, ℓ_1^+) as the one that gives the smallest m_{T2}. The distributions plotted in figure 6 sum over all the channels with the individual one weighted by the cross section, respectively. In the case of $M_\pi > 900\,\text{GeV}$, for the channels $\pi_6\pi_6^c$ and $\pi_6\bar{t}\bar{t}$, the m_{T2} criterion can achieve a 99% efficiency in order to get the correct combination. For the octet pair channel, the efficiency can be as high as 94%; while for the channel $\pi_6^c tt$, the efficiency is relatively lower, but still reaches 87%.

With the knowledge of the correct combinations of (b_1, ℓ_1^+) and (b_2, ℓ_2^+), we are capable of reconstructing the sextet mass from the leptonic top decay by calculating the four momenta of the two neutrinos. There are 6 unknown parameters and a four-fold solution will be achieved by analytically solving 2 linear equations from missing transverse momenta

[7] Of course we cannot determine the charge of the resonance and only infer that it is an anti-top from the fact that we look at a 4-top signature with two positively charged leptons in the final state.

[8] In the following, we discuss exclusively the l^+l^+ channel, but of course, for the l^-l^- channel the analogous discussion holds when replacing particles by anti-particles.

JHEP11(2015)201

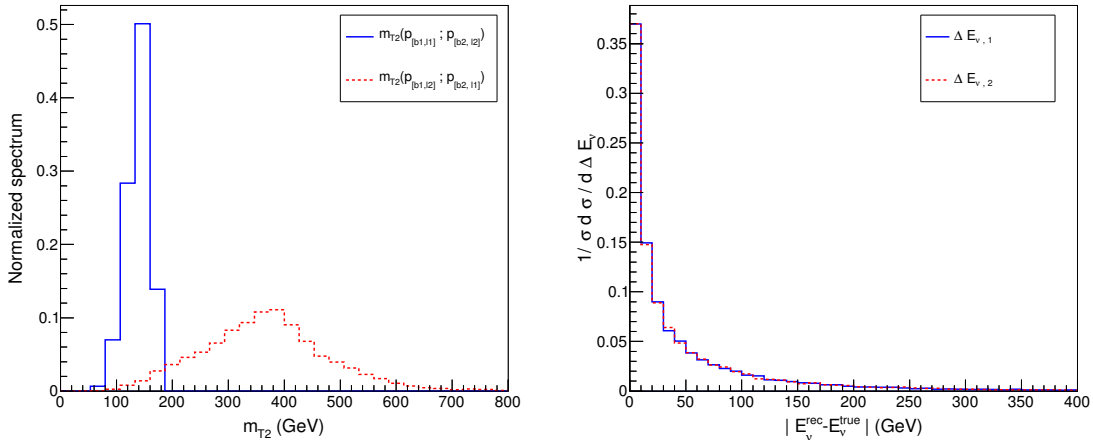

Figure 6. Left panel: m_{T2} distributions for two combinations of b-ℓ^+, the blue solid line corresponds to the correct combination and the red dashed line corresponds to the "wrong" one. The area under each distribution is normalized to be one. Right panel: distribution of ΔE_ν between the true one generated by a Monte Carlo simulation and the reconstructed solution.

and 4 nonlinear equations from the on-shell conditions of W mass and top quark mass [98, 99]. The fourth-degree polynomial for one neutrino energy can be expressed as:

$$c_0 + c_1 E_v + c_2 E_v^2 + c_3 E_v^3 + c_4 E_v^4 = 0 \tag{4.3}$$

where those coefficients c_i are complicated functions of m_W, m_t and momentum of leptons and bottom quarks. Solving this equation will lead to the possibility of 0, 2 or 4 real solutions and in this process, we shall apply an additional cut to require $E_\nu < 1500\,\text{GeV}$. Events with zero solutions will be discarded. Although the solutions satisfying the minimum kinematic constraints can all be generated, neutrinos in a certain energy range are more accessible at the LHC. Therefore we can resolve this ambiguity by choosing the solution with the smallest $|p_x|$ since the process being investigated does not carry large missing energy. In the right panel of figure 6, we show the statistical distribution for the difference in energy ΔE_ν of the reconstructed neutrino and the MC generated one. The possibility for either one of energy differences satisfying $\Delta E_{\nu,i} < 50\,\text{GeV}$ with $i = 1, 2$ reaches 80%, which validates our choice for the neutrinos with the smallest absolute value for the x-axis momentum. The mass of sextet is thus determined by the invariant mass of the reconstructed tt pair.

Figure 7 shows reconstructed invariant mass of the tt pair from the leptonic decay. We see that the channels with a π_6 in the final state generate a clear peak around the true mass (which will be smeared by detector effects), while processes with non-resonant tt pair, originating from the octet pair production or the tops associated with a single π_6^c, produce a continuum background. Setting a cut on the reconstructed invariant mass can thus allow to isolate the contribution of the $\pi_6 \to tt$ decays and reveal the presence of a sextet in the data.

JHEP11(2015)201

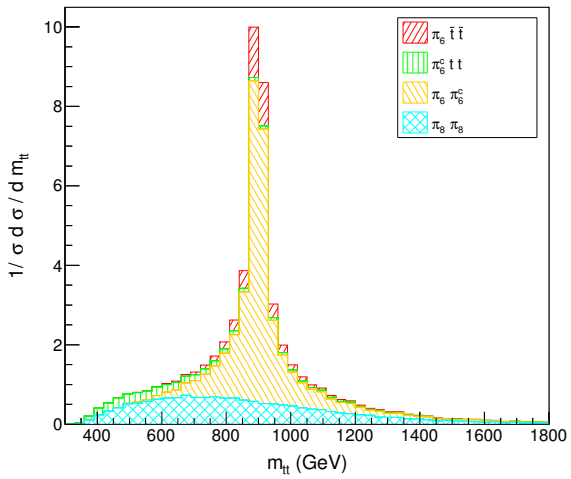

Figure 7. Staggered plot of the invariant mass m_{tt} distribution from dilepton decay for the case of $M_\pi = 900\,\text{GeV}$ and $a_R = 1$ for the channels $\pi_6\overline{tt}, \pi_6^c tt, \pi_6^c\pi_6$, and $\pi_8\pi_8$. The peak is reconstructed after passing the basic cuts and the b-tag efficiency is included.

A further invariant mass can be reconstructed from the hadronic $\overline{tt}$ pair.[9] For $m_{\overline{tt}}$, the processes $\pi_6^c\pi_6$ and $\pi_6^c tt$ yield a contribution which is peaked around M_π while $\pi_8\pi_8$ and $\pi_6\overline{tt}$ contribute with flat distributions. Using both mass invariants in parallel thus even in principle allows to directly determine the coupling a_R, as in $\pi_6^c\pi_6$ events, both the leptonic and the hadronic invariant masses reproduce M_π simultaneously, while $\pi_6\overline{tt}$ reconstructs leptonically but not hadronically and vice versa for $\pi_6^c tt$.[10] Here, we do not quantify the separation power of the direct measurement of a_R as its significance depends on the backgrounds, and in our analysis we can only include the true SM background, while the background from fake 2SSL events and 2SSL events which arise from charge mis-identification needs to be extracted from actual data. We just wish to point out that reconstructing the π_6 mass in two independent ways in principle allows for a direct measurement of a_R.

Also, the angular distributions of the leptons carry important information about their origin. One simple way to differentiate the sextet from the octet without boosting the lepton momenta is to use the opening angle between the 2SSL in the detector frame, which is defined as:

$$\cos\theta_{\ell_1^+\ell_2^+} = \frac{\vec{p}_{\ell_1}\cdot\vec{p}_{\ell_2}}{|\vec{p}_{\ell_1}|\,|\vec{p}_{\ell_2}|}\,. \tag{4.4}$$

In the case of a 2SSL from a π_6 decay, the opening angle tends to be large for two reasons. First, as $M_\pi \gtrsim 800$ GeV from Run I constraints already, the π_6 decays into two boosted tops which have a large opening angle as the π_6 itself will be dominantly produced at low

[9] This procedure has been carried out in ref. [75].

[10] An indirect measurement of a_R could also be obtained by comparing the mismatch of the number of events with a reconstructed tt resonance to the prediction of such events by QCD pair production of such events for the mass determined from the measurement.

JHEP11(2015)201

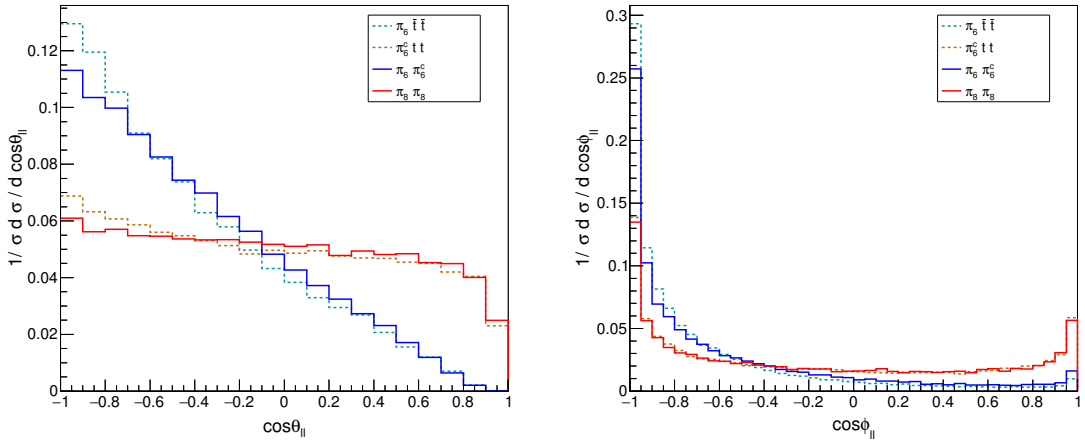

Figure 8. Left panel: dilepton opening angle distribution in the laboratory frame of the different $4t$ channels (and $M_\pi = 900$ GeV) after passing the basic cuts. Right panel: dileptonic azimuthal angle difference distribution in the laboratory frame for the same channels and $M_\pi = 900$ GeV, after passing the basic cuts.

boost (in single as well as in pair production). As the tops are highly boosted, their decay products (and in particular the leptons) are approximately collinear to the boost direction, and therefore also the 2SSL tend to have a large opening angle. Second, according to the lepton correlation with the top spin in the top decay, the lepton tends to move in the same direction as the top quark momentum for a pure t_R case. Thus, in the case that the two leptons are coming from one sextet resonance which in our model couples purely to right-handed tops, they are more likely to be back-to-back thus giving a maximal opening angle. For the other cases where the dilepton comes from unpolarised top quarks and/or from the decay of two different resonances, the opening angle distribution will be more spherical. The differential distribution $1/\sigma \cdot d\sigma/d\cos\theta_{\ell_1^+\ell_2^+}$ for a mass $M_\pi = 900$ GeV, shown in the left panel of figure 8, illustrates this fact. For larger M_π, the 2SSL opening angle increases even further for events with a π_6, as the tops arising from its decay are more boosted.

Alternatively (or in addition), one can use the difference in azimuthal angles $\phi_{\ell_1^+\ell_2^+}$ with $\vec{p}_{\ell_1}$ and $\vec{p}_{\ell_2}$ in the laboratory frame to trace the spin correlation between the two leptons. The advantage of this variable is that this information can be easily obtained at the LHC and at the same time it is sensitive to the polarisation of the top quarks. In analogy to the $t\bar{t}$ pair decay [100, 101], we define the azimuthal angle correlation in the scenario of 2SSL to be:

$$\cos\phi_{\ell_1^+\ell_2^+} = \frac{\vec{p}_{\ell_1}\cdot\vec{p}_{\ell_2} - p^z_{\ell_1} p^z_{\ell_2}}{|\vec{p}_{\ell_1}|\,|\vec{p}_{\ell_2}|} \tag{4.5}$$

In the right panel of figure 8, we plot the distribution of $1/\sigma\cdot d\sigma/d\cos\phi_{\ell_1^+\ell_2^+}$ for each channel, again for $M_\pi = 900$ GeV. In both cases — whether the 2SSL arises from a π_6 decay or not — the azimuthal angle difference peaks towards the back-to-back configuration, however the azimuthal angle asymmetry in the sextet channel is much more pronounced than in

JHEP11(2015)201

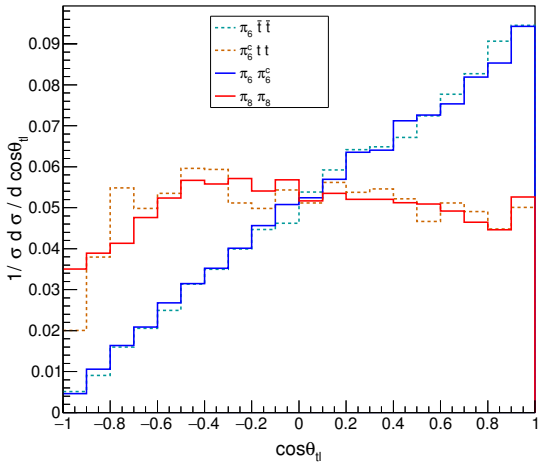

Figure 9. Leptonic angular distribution relative to the top quark momentum for the events with top quark reconstructed and passing the basic cut. Note that we also impose a mass window selection rule $|m_{tt} - 900\ \text{GeV}| < 100\ \text{GeV}$.

the octet channel. For the octet case, it is the momentum conservation which forces the 2 SSL coming from two different resonances to be back to back in the moving direction, while for the sextet case the two leptons from one resonance will also fly in the opposite direction due to the helicity conservation.

Apart from considering angular distributions in the laboratory frame, we are also considering angular distributions in the rest-frame of the tops in order to directly access the chirality of the tops produced. These distributions naively appear to be harder to access as the tops are highly boosted such that the angular resolution in the rest frame of the top are subject to large uncertainties but we nevertheless find that these distributions yield some sensitivity. In the case under study, the tops originating from the decays of the sextet are dominantly right-handed, while the tops from the octet and the ones associated to the singly produced sextet have mixed chirality. The chiral structure of the top quarks can be identified by using the leptonic angular distribution in the rest frame of the top quark: we can define $\theta_{t\ell}$ to be the angle between the lepton momentum and the chosen spin axis for the top quark, i.e. its spatial momentum in the rest frame of tt pair. The differential decay rate is simply described by [102–104]:

$$\frac{1}{\sigma}\frac{d\sigma}{d\cos\theta_{t\ell^+}} = \frac{1}{2}(1 + a\cos\theta_{t\ell^+}), \tag{4.6}$$

with $a = 1$ for a pure t_R and $a = -1$ for a pure t_L. In figure 9, we display the $\cos\theta_{t\ell^+}$ distributions for each channel for $M_\pi = 900$ GeV, where we boost the p_{ℓ^+} of the positive lepton into the rest frame of top quark and also boost the p_t into the rest frame of the tt pair cluster. For the cases $\pi_6 t\bar{t}$, $\pi_6\pi_6^c$, with the positive lepton ℓ^+ as a daughter particle from the scalar π_6, the events show a clear distribution of $(1+\cos\theta_{t\ell^+})$, which verifies that a sextet scalar only couples to right handed tops. On the other hand, for the other cases $\pi_6^c tt$ and $\pi_8\pi_8$, the distributions are substantially flatter.

JHEP11(2015)201

5 Conclusions

Fundamental composite electroweak dynamics (FCD) is an alternative way to build models of the electroweak interactions where the Higgs boson arises as a composite state of a confining dynamics with fermionic components. This approach allows to identify the light resonances one may expect in the low energy theory, thus providing a precious guidance in the construction of effective models of a composite Higgs. Requiring a fermionic UV completion leads to the immediate conclusion that one may well expect more scalar mesons than a Higgs-like singlet and the eaten Goldstone bosons. In particular, the requirement that the theory generates fermionic bound states (baryons) that carry colour generically imply the presence of coloured mesons in the spectrum, whose mass is linked to the mass of the baryons themselves. The baryons play the role of top partners in the partial compositeness paradigm by mixing linearly with the top (and bottom) to provide them a mass.

We focused on the scenario where the coloured scalars are lighter that the coloured baryons: in this case, they dominantly couple to top quarks via the mixing dictated by partial compositeness. We considered a charged sextet coupling to a di-top state, and real octet coupling to $t\bar{t}$. We then studied the phenomenology at the LHC, both Run I and II, by using of a simplified Lagrangian approach. Gauge invariance under the EW gauge group requires that the sextet couples dominantly to right handed tops with an unsuppressed (order 1) coupling. We thus considered both pair production of sextet and octet, and the single production of the sextet in association to an anti-top pair. All production channels give rise to 4-top final states, which are very well constrained by searches focusing on two same sign leptons, and one lepton plus jets. The searches at Run I on the full dataset provide a lower bound on the mass of the new scalars ranging from 800 GeV to 1.1 TeV. We then investigated the perspectives for Run II, and in particular the possibility of distinguishing the presence of a sextet in the same sign lepton search from the presence of an octet once a significant excess is detected. Same sign leptons are promising as they originate from the decay of a single resonance $\pi_6 \to tt \to bbl^+l^+ \not{E}_T$, thus giving a handle on the kinematics of the resonance. We illustrated three methods apt to single out the sextet from the signal. The first possibility is to reconstruct the resonance by fully reconstructing the leptonically decaying tops: we demonstrated that this can be done with very high efficiency by a simulation at particle level. Detector effects will smear the peak, however a distinction from the smooth distribution provided by the octet is possible. The other two methods rely on the angular distributions of the leptons, and rely on the fact that the sextet decays to two right handed tops (and not a $t\bar{t}$ pair). One method we presented relies on studying angular distributions between the two leptons in the laboratory frame, which are produced more back-to-back from the sextet decays then from other channels. The other method consists on studying the chirality of the leptonically decaying tops, showing a marked right-handed polarisation in the signal events from the sextet.

The set up we studied may be rather general, however we present an explicit model where such states are predicted. The model is based on a coset SU(4)/Sp(4) in the EW sector, giving rise to a Higgs-like state plus a singlet. QCD colour interactions are in-

JHEP11(2015)201

cluded by adding a second species of fundamental fermions, thus adding a global symmetry SU(6)/SO(6) which generates a neutral octet and a charged sextet as pseudo-Nambu-Goldstone bosons. We studied how the masses can be generated, showing that they can be naturally degenerate at the TeV scale. We further investigated the couplings to fermions arising via the partial compositeness couplings. Besides the aforementioned couplings to tops, the coloured mesons also couple to the top partners. Depending on the detailed spectrum, one may therefore expect decays of the top partners into the coloured scalars, thus weakening the bounds on vector-like top partners from present searches while at the same time boosting the production cross section of coloured scalars further. Another interesting possibility would be that the scalars (if heavier than the top partners) may decay into top partners, thus providing an additional production mechanism for them.

Acknowledgments

This work was supported by the National Research Foundation of Korea (NRF) grant funded by the Korea government (MEST) (No. 2012R1A2A2A01045722), the International Research and Development Program of the National Research Foundation of Korea (NRF) funded by the Ministry of Science, ICT and Future Planning (Grant number: 2015K1A3A1A21000234), and by the Basic Science Research Program through the National Research Foundation of Korea (NRF) funded by the ministry of Education, Science and Technology (No. 2013R1A1A1062597). We thank the France-Korea Particle Physics Lab (FKPPL) for partial support. AD is partially supported by Institut Universitaire de France. AP acknowledges IBS Korea for support under system code IBS-R017-D1-2015-a00. We also acknowledge partial support from the Labex-LIO (Lyon Institute of Origins) under grant ANR-10-LABX-66 and FRAMA (FR3127, Fédération de Recherche "André Marie Ampère").

A Pre-Yukawa coupling structures

The expansions for the 4 pre-Yukawa couplings read:

$$y_{5R} f\, \xi_R U_4^{(R)} \psi_5 = \frac{y_{5R} f}{\sqrt{2}} \left[t_R^c (T + X_{2/3}) \left(\sin\epsilon + \cos\epsilon \frac{h}{\sqrt{2}} \right) + i t_R^c \tilde{T}_5 \cos\epsilon \, \frac{\eta}{f} + \dots \right], \tag{A.1}$$

$$y_{5R} f\, \xi_R U_4^{(R)} \eta_5 = -\frac{y_{5R} f}{\sqrt{2}} \left[t_R^c (T^c + X_{2/3}^c) \sin\epsilon + \dots \right]; \tag{A.2}$$

$$y_{1R} f\, \xi_R U_4^{(R)} \psi_1 = y_{1R} f \left[t_R^c \tilde{T}_1 \left(\cos\epsilon - \sin\epsilon \frac{h}{\sqrt{2}} \right) + \dots \right], \tag{A.3}$$

$$y_{1R} f\, \xi_R U_4^{(R)} \eta_1 = y_{1R} f \left[t_R^c \tilde{T}_1^c \cos\epsilon + \dots \right]; \tag{A.4}$$

$$\begin{aligned} y_{5L} f\, \xi_L U_4^{(R)} \eta_5 = y_{5L} f \Big[& B^c b_L + T^c t_L \cos^2\frac{\epsilon}{2} - X_{2/3}^c t_L \sin^2\frac{\epsilon}{2} + \\ & - \frac{1}{2}(T^c + X_{2/3}^c) t_L \sin\epsilon \, \frac{h}{\sqrt{2}} + i \frac{1}{2} \tilde{T}_5^c t_L \sin\epsilon \frac{\eta}{f} + \dots \Big], \end{aligned} \tag{A.5}$$

$$y_{5L} f\, \xi_L U_4^{(R)} \psi_5 = y_{5L} f \left[X_{5/3} b_L + T t_L \sin^2\frac{\epsilon}{2} - X_{2/3} t_L \cos^2\frac{\epsilon}{2} + \dots \right]; \tag{A.6}$$

$$y_{1L} f\, \xi_R U_4^{(R)} \eta_1 = \frac{y_{1L} f}{\sqrt{2}} \left[\tilde{T}_1^c t_L \left(\sin\epsilon + \cos\epsilon \frac{h}{\sqrt{2}} \right) + \dots \right] , \tag{A.7}$$

$$y_{1L} f\, \xi_R U_4^{(R)} \psi_1 = \frac{y_{1L} f}{\sqrt{2}} \left[\tilde{T}_1 t_L \sin\epsilon + \dots \right] . \tag{A.8}$$

The couplings of the octet can be obtained from eq. (2.20) and eq. (2.21), and are proportional to the mass matrix (with $M_{5,1} = 0$):

$$g_{\pi_8 t_L t_R^c} = -i \frac{f}{\sqrt{2} f_6} \begin{pmatrix} 0 & y_{5L} \cos^2\frac{\epsilon}{2} & -y_{5L} \sin^2\frac{\epsilon}{2} & \frac{y_{1L}}{\sqrt{2}} \sin\epsilon & 0 \\ \frac{y_{5R}}{\sqrt{2}} \sin\epsilon & 0 & 0 & 0 & 0 \\ \frac{y_{5R}}{\sqrt{2}} \sin\epsilon & 0 & 0 & 0 & 0 \\ y_{1R} \cos\epsilon & 0 & 0 & 0 & 0 \\ 0 & 0 & 0 & 0 & 0 \end{pmatrix} , \tag{A.9}$$

in the gauge eigenstate basis. The couplings of the sextet can be written as:

$$g_{\pi_6 t_R^c t_R^c} = -i \frac{f}{2\sqrt{2} f_6} \begin{pmatrix} 0 & -\frac{y_{5R}}{\sqrt{2}} \sin\epsilon & -\frac{y_{5R}}{\sqrt{2}} \sin\epsilon & y_{1R} \cos\epsilon & 0 \\ -\frac{y_{5R}}{\sqrt{2}} \sin\epsilon & 0 & 0 & 0 & 0 \\ -\frac{y_{5R}}{\sqrt{2}} \sin\epsilon & 0 & 0 & 0 & 0 \\ y_{1R} \cos\epsilon & 0 & 0 & 0 & 0 \\ 0 & 0 & 0 & 0 & 0 \end{pmatrix} ; \tag{A.10}$$

$$g_{\pi_6^c t_L t_L} = -i \frac{f}{2\sqrt{2} f_6} \begin{pmatrix} 0 & y_{5L} \sin^2\frac{\epsilon}{2} & -y_{5L} \cos^2\frac{\epsilon}{2} & \frac{y_{1L}}{\sqrt{2}} \sin\epsilon & 0 \\ y_{5L} \sin^2\frac{\epsilon}{2} & 0 & 0 & 0 & 0 \\ -y_{5L} \cos^2\frac{\epsilon}{2} & 0 & 0 & 0 & 0 \\ \frac{y_{1L}}{\sqrt{2}} \sin\epsilon & 0 & 0 & 0 & 0 \\ 0 & 0 & 0 & 0 & 0 \end{pmatrix} . \tag{A.11}$$

For the bottom, in the basis $\{b, B\}$,

$$M_{\text{bottom}} = \begin{pmatrix} 0 & y_{5L} f \\ 0 & M_5 \end{pmatrix} , \tag{A.12}$$

and the coupling of the octet and sextet reads:

$$g_{\pi_8 b_L b_R^c} = -i \frac{f}{\sqrt{2} f_6} \begin{pmatrix} 0 & y_{5L} \\ 0 & 0 \end{pmatrix} , \quad g_{\pi_6^c b_L X_{5/3}} = -i \frac{f}{\sqrt{2} f_6} y_{5L} . \tag{A.13}$$

References

[1] S. Weinberg, *Implications of Dynamical Symmetry Breaking*, *Phys. Rev.* **D 13** (1976) 974 [INSPIRE].

JHEP11(2015)201

[2] S. Weinberg, *Implications of Dynamical Symmetry Breaking: An Addendum*, *Phys. Rev.* **D 19** (1979) 1277 [INSPIRE].

[3] L. Susskind, *Dynamics of Spontaneous Symmetry Breaking in the Weinberg-Salam Theory*, *Phys. Rev.* **D 20** (1979) 2619 [INSPIRE].

[4] D.B. Kaplan and H. Georgi, *SU(2) x U(1) Breaking by Vacuum Misalignment*, *Phys. Lett.* **B 136** (1984) 183 [INSPIRE].

[5] D.B. Kaplan, H. Georgi and S. Dimopoulos, *Composite Higgs Scalars*, *Phys. Lett.* **B 136** (1984) 187 [INSPIRE].

[6] H. Georgi, D.B. Kaplan and P. Galison, *Calculation of the Composite Higgs Mass*, *Phys. Lett.* **B 143** (1984) 152 [INSPIRE].

[7] T. Banks, *CONSTRAINTS ON* SU(2) *x U(1) BREAKING BY VACUUM MISALIGNMENT*, *Nucl. Phys.* **B 243** (1984) 125 [INSPIRE].

[8] H. Georgi and D.B. Kaplan, *Composite Higgs and Custodial* SU(2), *Phys. Lett.* **B 145** (1984) 216 [INSPIRE].

[9] M.J. Dugan, H. Georgi and D.B. Kaplan, *Anatomy of a Composite Higgs Model*, *Nucl. Phys.* **B 254** (1985) 299 [INSPIRE].

[10] R. Contino, Y. Nomura and A. Pomarol, *Higgs as a holographic pseudoGoldstone boson*, *Nucl. Phys.* **B 671** (2003) 148 [hep-ph/0306259] [INSPIRE].

[11] K. Agashe, R. Contino and A. Pomarol, *The Minimal composite Higgs model*, *Nucl. Phys.* **B 719** (2005) 165 [hep-ph/0412089] [INSPIRE].

[12] K. Agashe and R. Contino, *The Minimal composite Higgs model and electroweak precision tests*, *Nucl. Phys.* **B 742** (2006) 59 [hep-ph/0510164] [INSPIRE].

[13] M.A. Luty and T. Okui, *Conformal technicolor*, *JHEP* **09** (2006) 070 [hep-ph/0409274] [INSPIRE].

[14] A.V. Manohar and M.B. Wise, *Modifications to the properties of the Higgs boson*, *Phys. Lett.* **B 636** (2006) 107 [hep-ph/0601212] [INSPIRE].

[15] G.F. Giudice, C. Grojean, A. Pomarol and R. Rattazzi, *The Strongly-Interacting Light Higgs*, *JHEP* **06** (2007) 045 [hep-ph/0703164] [INSPIRE].

[16] B. Grinstein and M. Trott, *A Higgs-Higgs bound state due to new physics at a TeV*, *Phys. Rev.* **D 76** (2007) 073002 [arXiv:0704.1505] [INSPIRE].

[17] R. Barbieri, B. Bellazzini, V.S. Rychkov and A. Varagnolo, *The Higgs boson from an extended symmetry*, *Phys. Rev.* **D 76** (2007) 115008 [arXiv:0706.0432] [INSPIRE].

[18] G. Panico and A. Wulzer, *The Discrete Composite Higgs Model*, *JHEP* **09** (2011) 135 [arXiv:1106.2719] [INSPIRE].

[19] S. De Curtis, M. Redi and A. Tesi, *The 4D Composite Higgs*, *JHEP* **04** (2012) 042 [arXiv:1110.1613] [INSPIRE].

[20] R. Alonso, M.B. Gavela, L. Merlo, S. Rigolin and J. Yepes, *The Effective Chiral Lagrangian for a Light Dynamical "Higgs Particle"*, *Phys. Lett.* **B 722** (2013) 330 [*Erratum ibid.* **B 726** (2013) 926] [arXiv:1212.3305] [INSPIRE].

[21] R. Contino, M. Ghezzi, C. Grojean, M. Muhlleitner and M. Spira, *Effective Lagrangian for a light Higgs-like scalar*, *JHEP* **07** (2013) 035 [arXiv:1303.3876] [INSPIRE].

JHEP11(2015)201

[22] E. Katz, A.E. Nelson and D.G.E. Walker, *The Intermediate Higgs*, *JHEP* **08** (2005) 074 [hep-ph/0504252] [INSPIRE].

[23] B. Gripaios, A. Pomarol, F. Riva and J. Serra, *Beyond the Minimal Composite Higgs Model*, *JHEP* **04** (2009) 070 [arXiv:0902.1483] [INSPIRE].

[24] J. Mrazek, A. Pomarol, R. Rattazzi, M. Redi, J. Serra and A. Wulzer, *The Other Natural Two Higgs Doublet Model*, *Nucl. Phys.* **B 853** (2011) 1 [arXiv:1105.5403] [INSPIRE].

[25] R. Contino, L. Da Rold and A. Pomarol, *Light custodians in natural composite Higgs models*, *Phys. Rev.* **D 75** (2007) 055014 [hep-ph/0612048] [INSPIRE].

[26] C. Anastasiou, E. Furlan and J. Santiago, *Realistic Composite Higgs Models*, *Phys. Rev.* **D 79** (2009) 075003 [arXiv:0901.2117] [INSPIRE].

[27] G. Cacciapaglia and F. Sannino, *Fundamental Composite (Goldstone) Higgs Dynamics*, *JHEP* **04** (2014) 111 [arXiv:1402.0233] [INSPIRE].

[28] T.A. Ryttov and F. Sannino, *Ultra Minimal Technicolor and its Dark Matter TIMP*, *Phys. Rev.* **D 78** (2008) 115010 [arXiv:0809.0713] [INSPIRE].

[29] J. Galloway, J.A. Evans, M.A. Luty and R.A. Tacchi, *Minimal Conformal Technicolor and Precision Electroweak Tests*, *JHEP* **10** (2010) 086 [arXiv:1001.1361] [INSPIRE].

[30] J. Barnard, T. Gherghetta and T.S. Ray, *UV descriptions of composite Higgs models without elementary scalars*, *JHEP* **02** (2014) 002 [arXiv:1311.6562] [INSPIRE].

[31] G. Ferretti and D. Karateev, *Fermionic UV completions of Composite Higgs models*, *JHEP* **03** (2014) 077 [arXiv:1312.5330] [INSPIRE].

[32] G. Ferretti, *UV Completions of Partial Compositeness: The Case for a* SU(4) *Gauge Group*, *JHEP* **06** (2014) 142 [arXiv:1404.7137] [INSPIRE].

[33] L. Vecchi, *A "dangerous irrelevant" UV-completion of the composite Higgs*, arXiv:1506.00623 [INSPIRE].

[34] A. Hietanen, R. Lewis, C. Pica and F. Sannino, *Fundamental Composite Higgs Dynamics on the Lattice:* SU(2) *with Two Flavors*, *JHEP* **07** (2014) 116 [arXiv:1404.2794] [INSPIRE].

[35] A. Arbey, G. Cacciapaglia, H. Cai, A. Deandrea, S. Le Corre and F. Sannino, *Fundamental Composite Electroweak Dynamics: Status at the LHC*, arXiv:1502.04718 [INSPIRE].

[36] B. Bellazzini, C. Csáki and J. Serra, *Composite Higgses*, *Eur. Phys. J.* **C 74** (2014) 2766 [arXiv:1401.2457] [INSPIRE].

[37] G. Panico and A. Wulzer, *The Composite Nambu-Goldstone Higgs*, arXiv:1506.01961 [INSPIRE].

[38] B. Gripaios, *Composite Leptoquarks at the LHC*, *JHEP* **02** (2010) 045 [arXiv:0910.1789] [INSPIRE].

[39] R. Lewis, C. Pica and F. Sannino, *Light Asymmetric Dark Matter on the Lattice:* SU(2) *Technicolor with Two Fundamental Flavors*, *Phys. Rev.* **D 85** (2012) 014504 [arXiv:1109.3513] [INSPIRE].

[40] A. Hietanen, R. Lewis, C. Pica and F. Sannino, *Composite Goldstone Dark Matter: Experimental Predictions from the Lattice*, *JHEP* **12** (2014) 130 [arXiv:1308.4130] [INSPIRE].

JHEP11(2015)201

[41] F. Sannino, *Conformal Windows of SP(2N) and* SO(N) *Gauge Theories*, *Phys. Rev.* **D 79** (2009) 096007 [arXiv:0902.3494] [INSPIRE].

[42] S. Raby, S. Dimopoulos and L. Susskind, *Tumbling Gauge Theories*, *Nucl. Phys.* **B 169** (1980) 373 [INSPIRE].

[43] G. Cacciapaglia, H. Cai, T. Flacke, S.J. Lee, A. Parolini and H. Serôdio, *Anarchic Yukawas and top partial compositeness: the flavour of a successful marriage*, *JHEP* **06** (2015) 085 [arXiv:1501.03818] [INSPIRE].

[44] O. Matsedonskyi, G. Panico and A. Wulzer, *On the Interpretation of Top Partners Searches*, *JHEP* **12** (2014) 097 [arXiv:1409.0100] [INSPIRE].

[45] M. Backović, T. Flacke, S.J. Lee and G. Perez, *LHC Top Partner Searches Beyond the 2 TeV Mass Region*, *JHEP* **09** (2015) 022 [arXiv:1409.0409] [INSPIRE].

[46] R. Casalbuoni, S. De Curtis, D. Dominici and R. Gatto, *Effective Weak Interaction Theory with Possible New Vector Resonance from a Strong Higgs Sector*, *Phys. Lett.* **B 155** (1985) 95 [INSPIRE].

[47] R. Contino, D. Marzocca, D. Pappadopulo and R. Rattazzi, *On the effect of resonances in composite Higgs phenomenology*, *JHEP* **10** (2011) 081 [arXiv:1109.1570] [INSPIRE].

[48] B. Bellazzini, C. Csáki, J. Hubisz, J. Serra and J. Terning, *Composite Higgs Sketch*, *JHEP* **11** (2012) 003 [arXiv:1205.4032] [INSPIRE].

[49] H. Cai, *Higgs decay into a diphoton in the composite Higgs model*, *Phys. Rev.* **D 88** (2013) 035018 [arXiv:1303.3833] [INSPIRE].

[50] D. Pappadopulo, A. Thamm, R. Torre and A. Wulzer, *Heavy Vector Triplets: Bridging Theory and Data*, *JHEP* **09** (2014) 060 [arXiv:1402.4431] [INSPIRE].

[51] D. Greco and D. Liu, *Hunting composite vector resonances at the LHC: naturalness facing data*, *JHEP* **12** (2014) 126 [arXiv:1410.2883] [INSPIRE].

[52] H. Cai, *Higgs-Z-photon Coupling from Effect of Composite Resonances*, *JHEP* **04** (2014) 052 [arXiv:1306.3922] [INSPIRE].

[53] C.-Y. Chen, A. Freitas, T. Han and K.S.M. Lee, *Heavy Color-Octet Particles at the LHC*, *JHEP* **05** (2015) 135 [arXiv:1410.8113] [INSPIRE].

[54] T. Han, I. Lewis and Z. Liu, *Colored Resonant Signals at the LHC: Largest Rate and Simplest Topology*, *JHEP* **12** (2010) 085 [arXiv:1010.4309] [INSPIRE].

[55] H. Zhang, E.L. Berger, Q.-H. Cao, C.-R. Chen and G. Shaughnessy, *Color Sextet Vector Bosons and Same-Sign Top Quark Pairs at the LHC*, *Phys. Lett.* **B 696** (2011) 68 [arXiv:1009.5379] [INSPIRE].

[56] ATLAS collaboration, *Search for strongly produced superpartners in final states with two same sign leptons with the ATLAS detector using 21 fb-1 of proton-proton collisions at* $\sqrt{s}$*=8 TeV*, ATLAS-CONF-2013-007 (2013).

[57] ATLAS collaboration, *Search for supersymmetry at* $\sqrt{s}$*=8 TeV in final states with jets and two same-sign leptons or three leptons with the ATLAS detector*, *JHEP* **06** (2014) 035 [arXiv:1404.2500] [INSPIRE].

[58] ATLAS collaboration, *Search for strong production of supersymmetric particles in final states with missing transverse momentum and at least three b-jets using 20.1* fb^{-1} *of pp collisions at* $\sqrt{s}$ *= 8 TeV with the ATLAS Detector*, ATLAS-CONF-2013-061 (2013).

JHEP11(2015)201

[59] ATLAS collaboration, *Search for new phenomena in final states with large jet multiplicities and missing transverse momentum at $\sqrt{s}$=8 TeV proton-proton collisions using the ATLAS experiment*, *JHEP* **10** (2013) 130 [*Erratum ibid.* **1401** (2014) 109] [arXiv:1308.1841] [INSPIRE].

[60] CMS collaboration, *Search for new physics in events with same-sign dileptons and jets in pp collisions at $\sqrt{s}$ = 8 TeV*, *JHEP* **01** (2014) 163 [*Erratum ibid.* **1501** (2015) 014] [arXiv:1311.6736] [INSPIRE].

[61] CMS collaboration, *Search for supersymmetry in pp collisions at $\sqrt{s}$=8 TeV in events with a single lepton, large jet multiplicity and multiple b jets*, *Phys. Lett.* **B 733** (2014) 328 [arXiv:1311.4937] [INSPIRE].

[62] CMS Collaboration, *Search for supersymmetry in pp collisions at $\sqrt{s}$ = 8 TeV in events with three leptons and at least one b-tagged jet*, CMS-PAS-SUS-13-008 (Search for supersymmetry in pp collisions at $\sqrt{s}$ = 8 TeV in events with three leptons and at least one b-tagged jet).

[63] CMS collaboration, *Search for new physics in the multijet and missing transverse momentum final state in proton-proton collisions at $\sqrt{s}$= 8 TeV*, *JHEP* **06** (2014) 055 [arXiv:1402.4770] [INSPIRE].

[64] C. Bini, R. Contino and N. Vignaroli, *Heavy-light decay topologies as a new strategy to discover a heavy gluon*, *JHEP* **01** (2012) 157 [arXiv:1110.6058] [INSPIRE].

[65] K. Agashe, R. Contino, L. Da Rold and A. Pomarol, *A Custodial symmetry for $Zb\bar{b}$*, *Phys. Lett.* **B 641** (2006) 62 [hep-ph/0605341] [INSPIRE].

[66] J. Serra, *Beyond the Minimal Top Partner Decay*, *JHEP* **09** (2015) 176 [arXiv:1506.05110] [INSPIRE].

[67] A. Anandakrishnan, J.H. Collins, M. Farina, E. Kuflik and M. Perelstein, *Odd Top Partners at the LHC*, arXiv:1506.05130 [INSPIRE].

[68] G.F. Giudice, B. Gripaios and R. Sundrum, *Flavourful Production at Hadron Colliders*, *JHEP* **08** (2011) 055 [arXiv:1105.3161] [INSPIRE].

[69] L. Calibbi, Z. Lalak, S. Pokorski and R. Ziegler, *Universal Constraints on Low-Energy Flavour Models*, *JHEP* **07** (2012) 004 [arXiv:1204.1275] [INSPIRE].

[70] G. Isidori, Y. Nir and G. Perez, *Flavor Physics Constraints for Physics Beyond the Standard Model*, *Ann. Rev. Nucl. Part. Sci.* **60** (2010) 355 [arXiv:1002.0900] [INSPIRE].

[71] F. Bazzocchi, U. De Sanctis, M. Fabbrichesi and A. Tonero, *Quark contact interactions at the LHC*, *Phys. Rev.* **D 85** (2012) 114001 [arXiv:1111.5936] [INSPIRE].

[72] O. Domenech, A. Pomarol and J. Serra, *Probing the SM with Dijets at the LHC*, *Phys. Rev.* **D 85** (2012) 074030 [arXiv:1201.6510] [INSPIRE].

[73] SUPER-KAMIOKANDE collaboration, K. Abe et al., *The Search for $n - \bar{n}$ oscillation in Super-Kamiokande I*, *Phys. Rev.* **D 91** (2015) 072006 [arXiv:1109.4227] [INSPIRE].

[74] R.N. Mohapatra, *Neutron-Anti-Neutron Oscillation: Theory and Phenomenology*, *J. Phys.* **G 36** (2009) 104006 [arXiv:0902.0834] [INSPIRE].

[75] C.-R. Chen, W. Klemm, V. Rentala and K. Wang, *Color Sextet Scalars at the CERN Large Hadron Collider*, *Phys. Rev.* **D 79** (2009) 054002 [arXiv:0811.2105] [INSPIRE].

JHEP11(2015)201

[76] T. Han, I. Lewis and T. McElmurry, *QCD Corrections to Scalar Diquark Production at Hadron Colliders*, *JHEP* **01** (2010) 123 [arXiv:0909.2666] [INSPIRE].

[77] E.L. Berger, Q.-H. Cao, C.-R. Chen, G. Shaughnessy and H. Zhang, *Color Sextet Scalars in Early LHC Experiments*, *Phys. Rev. Lett.* **105** (2010) 181802 [arXiv:1005.2622] [INSPIRE].

[78] M. Battaglia and G. Servant, *Four-top production and $t\bar{t}$ + missing energy events at multi TeV e^+e^- colliders*, *Nuovo Cim.* **C 033N2** (2010) 203 [arXiv:1005.4632] [INSPIRE].

[79] T. Gregoire, E. Katz and V. Sanz, *Four top quarks in extensions of the standard model*, *Phys. Rev.* **D 85** (2012) 055024 [arXiv:1101.1294] [INSPIRE].

[80] G. Cacciapaglia, R. Chierici, A. Deandrea, L. Panizzi, S. Perries and S. Tosi, *Four tops on the real projective plane at LHC*, *JHEP* **10** (2011) 042 [arXiv:1107.4616] [INSPIRE].

[81] J.A. Aguilar-Saavedra and J. Santiago, *Four tops and the $t\bar{t}$ forward-backward asymmetry*, *Phys. Rev.* **D 85** (2012) 034021 [arXiv:1112.3778] [INSPIRE].

[82] A. Deandrea and N. Deutschmann, *Multi-tops at the LHC*, *JHEP* **08** (2014) 134 [arXiv:1405.6119] [INSPIRE].

[83] ATLAS collaboration, *Search for exotic same-sign dilepton signatures (b' quark, $T_{5/3}$ and four top quarks production) in 4.7/fb of pp collisions at $\sqrt{s} = 7$ TeV with the ATLAS detector*, ATLAS-CONF-2012-130 (2012).

[84] CMS collaboration, *Search for standard model four top quark production at 8 TeV in the lepton + jets channel*, CMS-PAS-TOP-13-012 (2013).

[85] ATLAS collaboration, *Search for anomalous production of events with same-sign dileptons and b jets in 14.3 fb^{-1} of pp collisions at $\sqrt{s} = 8$ TeV with the ATLAS detector*, ATLAS-CONF-2013-051 (2013).

[86] CMS collaboration, *Search for Standard Model Production of Four Top Quarks in the Lepton + Jets Channel in pp Collisions at $\sqrt{s} = 8$ TeV*, *JHEP* **11** (2014) 154 [arXiv:1409.7339] [INSPIRE].

[87] ATLAS collaboration, *Analysis of events with b-jets and a pair of leptons of the same charge in pp collisions at $\sqrt{s} = 8$ TeV with the ATLAS detector*, *JHEP* **10** (2015) 150 [arXiv:1504.04605] [INSPIRE].

[88] ATLAS collaboration, *Search for production of vector-like quark pairs and of four top quarks in the lepton-plus-jets final state in pp collisions at $\sqrt{s} = 8$ TeV with the ATLAS detector*, *JHEP* **08** (2015) 105 [arXiv:1505.04306] [INSPIRE].

[89] CMS collaboration, *Search for new physics in events with same-sign dileptons and b jets in pp collisions at $\sqrt{s} = 8$ TeV*, *JHEP* **03** (2013) 037 [*Erratum ibid.* **1307** (2013) 041] [arXiv:1212.6194] [INSPIRE].

[90] CMS collaboration, *Search for new physics in events with same-sign dileptons and jets in pp collisions at $\sqrt{s} = 8$ TeV*, *JHEP* **01** (2014) 163 [*Erratum ibid.* **1501** (2015) 014] [arXiv:1311.6736] [INSPIRE].

[91] C. Degrande, B. Fuks, V. Hirschi, J. Proudom and H.-S. Shao, *Automated next-to-leading order predictions for new physics at the LHC: the case of colored scalar pair production*, *Phys. Rev.* **D 91** (2015) 094005 [arXiv:1412.5589] [INSPIRE].

[92] J. Alwall, R. Frederix, S. Frixione, V. Hirschi, F. Maltoni, O. Mattelaer et al., *The automated computation of tree-level and next-to-leading order differential cross sections and*

JHEP11(2015)201

their matching to parton shower simulations, *JHEP* **07** (2014) 079 [arXiv:1405.0301] [INSPIRE].

[93] A.D. Martin, W.J. Stirling, R.S. Thorne and G. Watt, *Parton distributions for the LHC*, *Eur. Phys. J.* **C 63** (2009) 189 [arXiv:0901.0002] [INSPIRE].

[94] ATLAS collaboration, *A search for $t\bar{t}$ resonances using lepton-plus-jets events in proton-proton collisions at $\sqrt{s} = 8$ TeV with the ATLAS detector*, *JHEP* **08** (2015) 148 [arXiv:1505.07018] [INSPIRE].

[95] CMS collaboration, *Search for Resonant $\mathrm{t\bar{t}}$ Production in Proton-Proton Collisions at $\sqrt{s}$ = 8 TeV*, arXiv:1506.03062 [INSPIRE].

[96] A. Barr, C. Lester and P. Stephens, *m(T2): The Truth behind the glamour*, *J. Phys.* **G 29** (2003) 2343 [hep-ph/0304226] [INSPIRE].

[97] H.-C. Cheng and Z. Han, *Minimal Kinematic Constraints and m(T2)*, *JHEP* **12** (2008) 063 [arXiv:0810.5178] [INSPIRE].

[98] L. Sonnenschein, *Analytical solution of ttbar dilepton equations*, *Phys. Rev.* **D 73** (2006) 054015 [*Erratum ibid.* **D 78** (2008) 079902] [hep-ph/0603011] [INSPIRE].

[99] Y. Bai and Z. Han, *Top-antitop and Top-top Resonances in the Dilepton Channel at the CERN LHC*, *JHEP* **04** (2009) 056 [arXiv:0809.4487] [INSPIRE].

[100] G. Mahlon and S.J. Parke, *Spin Correlation Effects in Top Quark Pair Production at the LHC*, *Phys. Rev.* **D 81** (2010) 074024 [arXiv:1001.3422] [INSPIRE].

[101] W. Bernreuther and Z.-G. Si, *Distributions and correlations for top quark pair production and decay at the Tevatron and LHC.*, *Nucl. Phys.* **B 837** (2010) 90 [arXiv:1003.3926] [INSPIRE].

[102] M. Jezabek and J.H. Kuhn, *Lepton Spectra from Heavy Quark Decay*, *Nucl. Phys.* **B 320** (1989) 20 [INSPIRE].

[103] G. Mahlon and S.J. Parke, *Angular correlations in top quark pair production and decay at hadron colliders*, *Phys. Rev.* **D 53** (1996) 4886 [hep-ph/9512264] [INSPIRE].

[104] T. Stelzer and S. Willenbrock, *Single top quark production via $q\bar{q} \to t\bar{b}$*, *Phys. Lett.* **B 357** (1995) 125 [hep-ph/9505433] [INSPIRE].

JHEP11(2015)201